Enhancement of Nucleate Pool Boiling Heat Transfer with Surfactant

K. M. Tanvir Ahmmed

MASTER OF SCIENCE IN ENGINEERING

(CHEMICAL)

Department of Chemical Engineering

BANGLADESH UNIVERSITY OF ENGINEERING AND TECHNOLOGY

DHAKA, BANGLADESH

December, 2011

Enhancement of Nucleate Pool Boiling Heat Transfer with Surfactant

By

K. M. Tanvir Ahmmed

MASTER OF SCIENCE IN ENGINEERING

(CHEMICAL)

Department of Chemical Engineering

BANGLADESH UNIVERSITY OF ENGINEERING AND TECHNOLOGY

December, 2011

Certification of Thesis Work

The thesis titled "Enhancement of Nucleate Pool Boiling Heat Transfer with Surfactant" submitted by K. M. Tanvir Ahmmed Roll No: 0409022007 has been accepted as satisfactory in partial fulfillment for the degree of Master of Science in Engineering (Chemical) on December 5, 2011.

1. _____
   Dr. Syeda Sultana Razia — Chairman
   Associate Professor
   Department of Chemical Engineering
   BUET, Dhaka.

2. _____
   Dr. Dil Afroza Begum — Member (Ex-officio)
   Professor and Head
   Department of Chemical Engineering
   BUET, Dhaka.

3. _____
   Sirajul Haque Khan — Member
   Associate Professor
   Department of Chemical Engineering
   BUET, Dhaka.

4. _____
   Dr. M. Imtiaz Hossain — Member (External)
   Vice-Chancellor
   IUT
   Board Bazar, Gazipur.

Candidate's Declaration

It is hereby declared that this thesis or any part of it has not been submitted elsewhere for the award of any degree or diploma.

_____

K. M. Tanvir Ahmmed

Abstract

Nucleate boiling is the preferred mode of boiling. An experimental setup for studying nucleate pool boiling of water with surfactant additive is developed. Sodium oleate is used as surfactant additive. Saturated nucleate pool boiling of both water and water with sodium oleate on a horizontal cylindrical heater surface has been investigated experimentally. Cartridge type electric heater with provision of surface temperature measurement is employed for heat generation. Change of heat flux with wall superheat is measured and change of heat transfer coefficient with wall superheat is calculated. The experimental results show that a small amount of surfactant enhances the heat transfer coefficient significantly. At low surfactant concentrations, heat transfer coefficient increases with increasing surfactant concentration in water. The maximum heat transfer enhancement is found to be at 250 ppm of sodium oleate solution. By adding more surfactant to water, heat transfer coefficient is found to be lowered. Surface tension of different concentration of sodium oleate solutions is measured. It is observed that the maximum heat transfer coefficient is obtained at a surfactant concentration that corresponds to the critical micelle concentration (cmc) of the surfactant/water solution.

Acknowledgements

First, I would like to express my sincere thanks to Dr. Syeda Sultana Razia for proposing this research topic. I would like to thank her for her valuable suggestions, excellent guidance, support, encouragement, and supervision that made this dissertation possible.

I am also thankful to the committee members for their valuable suggestions. Also, the valuable communications with Mr. Sirajul Haque Khan, Associate Professor, Department of Chemical Engineering, BUET on experimental setup, the generous help of Dr. Mahbub Razzaq, Professor, Department of Mechanical Engineering, BUET on the surface roughness measurement and, Mr. Sumon of Atomic Energy Center, Dhaka on the optical microscope images, are gratefully acknowledged. I would like to express my gratitude to Iftheker Ahmed Khan of South Carolina State University, USA for providing me a great number of literatures.

I would like to gratefully acknowledge Mr. Mahbub of Chemical Engineering Department, BUET for his cooperation with purchase of materials and chemicals, and setting up the experimental rig.

Acknowledgements are also made for the help rendered by the staff of the Chemical Engineering Department, BUET especially Mr. Abdul Mannan, Mr. Imran, Mr. Shafiullah, and Mr. John Biswas for their help during the research work.

Finally, I would like to thank all my colleagues and all my friends for their support during the research work.

Table of Contents

List of Figures

List of Tables

Nomenclature

c	Specific heat	J/kg.°C
d	Diameter	m
F	Force	N
g	Acceleration due to gravity	m/s^2
g_c	Conversion factor	
h	Heat transfer coefficient	$W/m^2.°C$
h_{fg}	Heat of vaporization	J/kg
k	Thermal conductivity	W/m.°C
p	Pressure	Pa
q''	Heat flux	W/m^2
α	Thermal diffusivity	m^2/s
θ	Contact angle	°
μ	Dynamic viscosity	cP
ρ	Density	kg/m^3
ΔT_e	Excess Temperature	°C
σ	Surface tension	mN/m

1. INTRODUCTION

1.1 Background

Nucleate boiling is the most efficient mode of boiling. Various fields of application of nucleate boiling can be found in traditional industries such as different energy conversion system, heat exchange system, refrigeration and heat pump system, air-conditioning, chemical thermal process, geo-thermal power plants. Its application can also be found in highly specialized fields such as cooling of high-energy-density electronic components, micro-fabricated fluidic system, the thermal control of aerospace station, evaporation in heat pipes, bioengineering reactors etc.

In boiling heat transfer, it is usually desirable to transfer the largest possible amount of heat with the smallest possible temperature difference between the heating surface and the boiling liquid, and to maximize the critical heat flux. Study of the enhancement of boiling heat transfer has become one of the fastest growing research areas of recent years [1]. This growth has been driven by the need to improve boiling heat transfer in high heat-flux devices (for example, in electronic component cooling) and in reducing the size and cost of equipment in chemical, refrigeration, and other types of plants. Various enhancement techniques have been developed over the past decades to fulfill these criteria [2,3].

Addition of small amount of surfactant to liquid, as an enhancement technique, shows a significant enhancement in pool boiling heat transfer [4,5,6,7]. Enhancement of nucleate pool boiling heat transfer with surfactant can lead to a significant increase in power level of boilers and boiling water nuclear reactors without increasing their size and operating temperature. One interesting field of application of surfactant enhanced heat transfer is in desalination of seawater, which is becoming essential in some arid regions. Sephton [8] in 1974 showed that addition of small amounts of surfactants to seawater can substantially enhance the boiling process, and reduce the price of the desalinated water to an acceptable level. As the environmental impact of surfactants was not known at that time, the research was discontinued.

Yang [9] pointed out that from an engineering point of view, it is desirable that the results of surfactant effect on boiling heat transfer can be analyzed, generalized and formulated into a more convenient form for calculations. However, only tentative criteria for a given surfactant as a competent additive in enhancing nucleate boiling heat transfer of water are available at present. The current state of research is far from a systematic theory or explanation for the enhancement of boiling heat transfer caused by surfactant additives. Further research should be conducted before the problems can be elucidated and the practical applications of surfactant additives in commercial plants are possible. Previous studies have shown that surfactants at low concentrations can enhance nucleate boiling heat transfer significantly but the mechanism was not understood properly. Recently, a number of studies have also been carried out to understand the mechanisms of nucleate boiling with surfactants, which generally include the effect of physical properties on boiling behavior, nucleation process and bubble dynamics. However, much fundamental work is needed for knowing both academic and practical aspects of boiling with surfactants. The recent state of the art review by Cheng et al. concluded that experiments of nucleate pool boiling of aqueous surfactant solution should be further emphasized to understand the boiling phenomena [10].

1.2. Objectives of the Study

The objectives of this study are

- To setup an experimental rig to study pool boiling phenomena.
- To generate boiling curves for water and water with surfactants.
- To interpret the boiling behavior in water and water with surfactant and enhancement due to the addition of surfactant to water.

1.3 Scope of the Study

This study employed a cartridge type cylindrical heater as a heating surface. The selection of heater was dictated by high heat-flux delivery and surface temperature measurement provision.

Sodium oleate is used as the surfactant because it depresses the surface tension significantly, it is commercially available as one of the raw materials for soap industry, and no considerable experimental study is available in literature.

1.4 Thesis Organization

In the following chapters the study is organized as follows

Chapter 2 provides a literature review of nucleate pool boiling and includes the different enhancement techniques of boiling heat transfer. Heat transfer enhancement with surfactant additives discussed in detail. Overview of surfactants is also presented.

Chapter 3 describes the experimental setup and methodology of the experiments.

Chapter 4 presents the results. The obtained results are also discussed in this chapter.

Chapter 5 states the concluding remarks of this study. Recommendations for future works are also presented.

2. LITERATURE REVIEW

2.1 Boiling Heat Transfer

When the temperature of a liquid at a specified pressure rises to its saturation temperature T_{sat} at that pressure, boiling occurs. A precise definition of boiling is presented by Hewitt [1], and Collier and Thome [11]. Boiling is the process of addition of heat to a liquid in such a way that vapor generation occurs. There are two basic types of boiling: *pool boiling* and *forced convection boiling*. Boiling on a heating surface submerged in an initially quiescent liquid is termed as pool boiling. In contrast, when the boiling occurs under forced-flow condition it is termed as flow boiling or forced convection boiling. Pool boiling and flow boiling are further classified as *subcooled boiling* and *saturated boiling*. When the temperature of the liquid is below the saturation temperature T_{sat}, it is said to be subcooled boiling or local boiling. If the liquid is at the saturation temperature then it is called saturated boiling or bulk boiling.

The phenomenon of boiling heat transfer is much more complex than that of convection heat transfer without phase change. This is because in addition to all the variables associated with convection heat transfer, other variables associated with phase change are also relevant for boiling heat transfer [12]. As a large number of variables are involved in boiling heat transfer neither general equation describing the boiling process nor the general correlation of boiling heat transfer data are available. Due to the importance of boiling heat transfer as well as the intellectual challenge made this field of study a flourishing one for the last 60 years. According to Bergles an accumulated literature of around 30,000 publications and 50 text books on boiling are in place already and around 1000 papers are coming out in each year [13]. In this literature review, an understanding of physical conditions associated with saturated nucleate pool boiling will be presented. And, the enhancement techniques, particularly surfactant effect will be focused.

2.2 Pool Boiling

Due to extensive research effort, the mechanism of pool boiling is relatively well understood. However, it is still not possible to predict the heat transfer characteristics for this simplest of boiling systems with the precision associated with single-phase systems [13]. The first complete characteristics of pool boiling were depicted by Nukiyama [14]. He boiled saturated water with a horizontal Nichrome wire which acted both as electric heater and resistance thermometer.

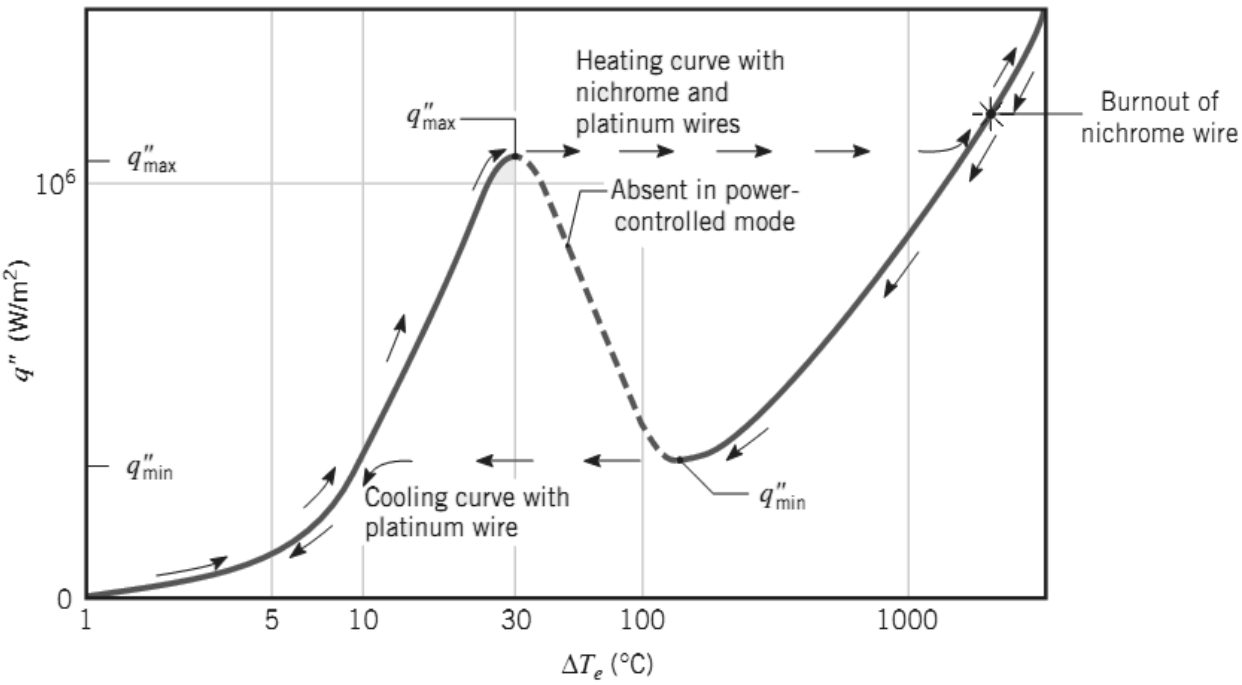

Fig. 2.1: Nukiyama's boiling curve for saturated water at atmospheric pressure.

The result of his experiment is shown in the *boiling curve* of Fig. 2.1, where the heat flux is plotted as a function of temperature difference between the heater surface and the saturation temperature of the liquid. This temperature difference, ΔT_e, is termed as the *excess temperature* or *wall superheat*. As the power to the wire increased, the heat flux was also increased but the wall superheat increased relatively little. This follows the heating curve of Fig. 2.1. Suddenly at a particular high heat flux the wire abruptly melted. This abrupt melting is termed as *burnout*. Then he used a platinum wire and at the same limiting heat

flux the wall superheat was very high that turned the wire white-hot. When he reduced the power the variation of ΔT_e with q'' followed the cooling curve of Fig. 2.1. This type of arrangement is termed *power-controlled heating*, wherein the wire temperature T_s (hence the excess temperature ΔT_e) is the dependent variable and the power setting (hence the heat flux q'') is the independent variable. Nukiyama believed that the hysteresis effect of Fig. 2.1 was a consequence of the power-controlled method of heating, where ΔT_e is a dependent variable. He also believed that by using a heating process permitting the independent control of ΔT_e, the missing (dashed) portion of the curve could be obtained.

In 1937, Drew and Mueller [15] succeeded in making ΔT_e the independent variable by boiling organic liquids outside a tube. Steam was allowed to condense inside the tube at an elevated pressure. The steam saturation temperature and hence the tube-wall temperature - was varied by controlling the steam pressure. This permitted them to obtain a few scattered data that seemed to bear out Nukiyama's conjecture. Measurements of this kind are inherently hard to make accurately.

2.3 Pool Boiling Regimes

Different boiling regimes in a typical case of pool boiling in saturated water at atmospheric pressure are delineated in Fig. 2.2. These boiling regimes, depicted in the curve, were observed by previous researchers, namely, Nukiyama [14], Drew and Mueller [15], and Farber and Scorah [16]. An understanding of the underlying physical mechanisms can be gained by examining the different modes, or regimes, of pool boiling. Boiling process occurs when the surface temperature, T_s exceeds the saturation temperature T_{sat} corresponding to the liquid pressure. Heat is transferred from the solid surface to the liquid, and the appropriate form of Newton's law of cooling is

$$q'' = h\,(T_s - T_{sat}) = h\,\Delta T_e \tag{2.1}$$

From Equation 2.1 we note that q'' depends on the convection coefficient h, as well as on the excess temperature ΔT_e. Different boiling regimes are explained according to the value of ΔT_e. A representation of the regimes is shown in Fig. 2.3.

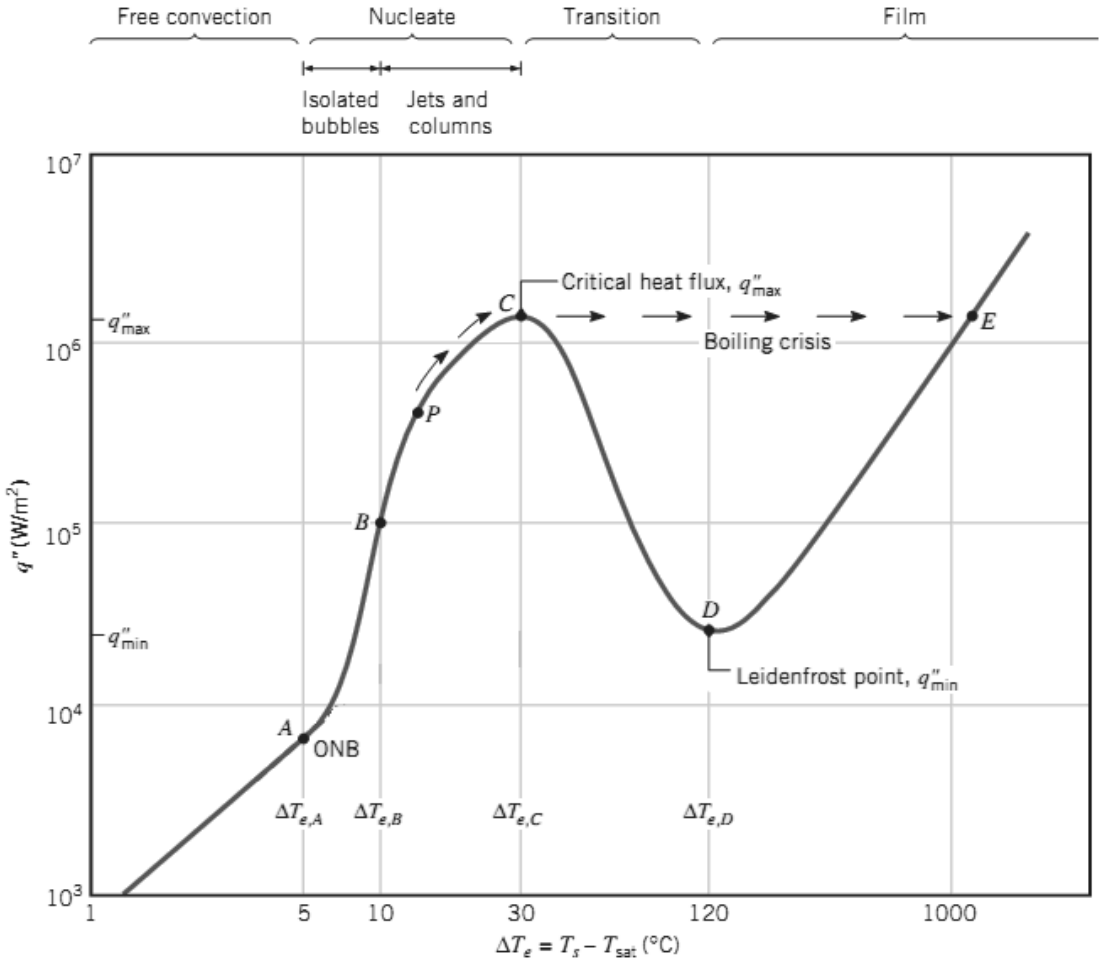

Fig. 2.2: Typical boiling curve for saturated water at atmospheric pressure[17].

2.3.1 Free convection boiling

The region corresponding to $\Delta T_e \leq \Delta T_{e,A}$ in Fig. 2.2 is termed as free convection boiling. In this region the surface temperature is somewhat above the saturation temperature in order to sustain bubble formation. As the excess temperature is increased, bubble inception will eventually occur, but below point A (referred to as the *onset of nucleate boiling*, ONB), fluid motion is determined principally by free convection effects.

2.3.2 Nucleate boiling

Nucleate boiling exists in the range $\Delta T_{e,A} \leq \Delta T_e \leq \Delta T_{e,C}$. In this range, two different flow regimes are observed. In region A–B, isolated bubbles form at nucleation sites and separate

from the surface. In the *isolated bubble regime*, most of the heat is transferred from the heating surface to the surrounding liquid by a vapor-liquid exchange action [18]. As vapor bubbles form and grow on the heating surface, they push hot liquid from the vicinity of the surface into the colder bulk of the liquid. In addition, intense micro-convection currents are set up as vapor bubbles are emitted and colder liquid from the bulk rushes toward the surface to fill the void. In this regime most of the heat exchange is through direct transfer from the surface to liquid in motion at the surface, and not through the vapor bubbles rising from the surface.

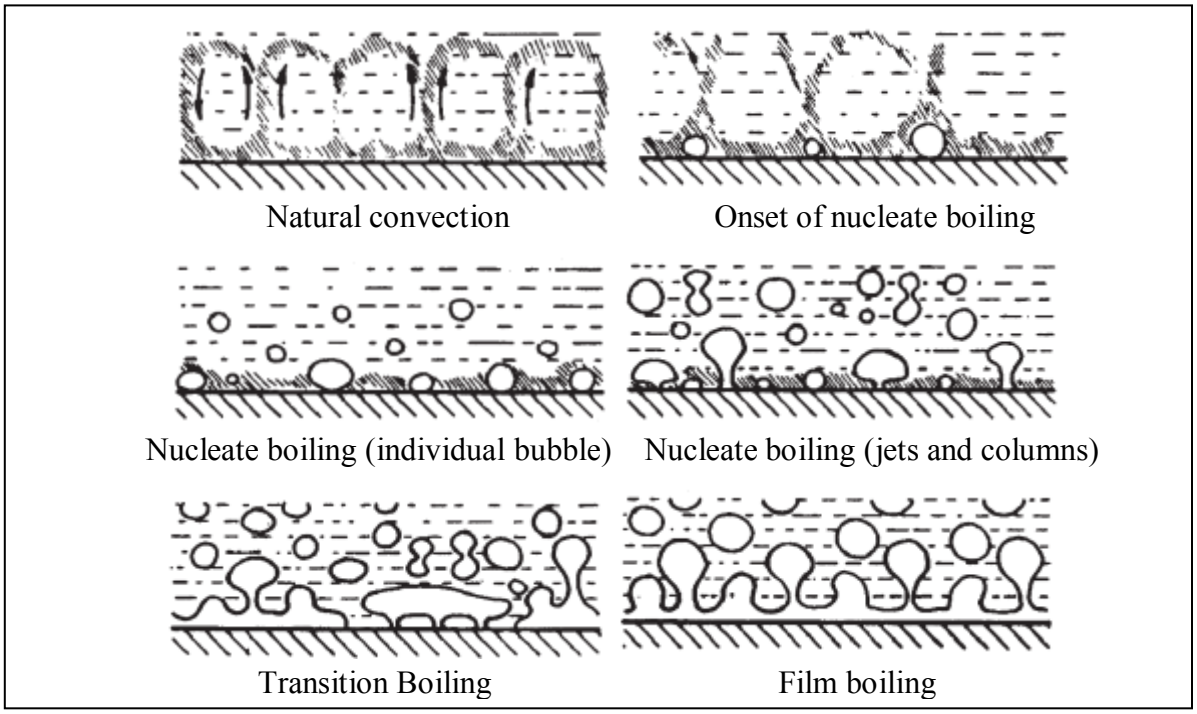

Fig. 2.3: Different pool boiling regimes

As ΔT_e is increased beyond $\Delta T_{e,B}$, more nucleation sites become active and increased bubble formation causes bubble interference and coalescence. The vapor escapes as jets or columns, which subsequently merge into slugs of the vapor. The region B to C is termed as *jets and columns regime*. Interference between the densely populated bubbles inhibits the motion of liquid near the surface. The maximum heat flux, q''_{max} , is usually termed the *critical heat flux(CHF)* or *departure from nucleate boiling (DNB)*, and in water at atmospheric pressure it exceeds 1 MW/m^2[17]. After this point for power-controlled apparatus *boiling crisis* arises. The critical heat fluxes for different metals are given in Table A.2.

At the point of this maximum, considerable vapor is being formed, making it difficult for liquid to continuously wet the surface. Because high heat transfer rates and convection coefficients are associated with small values of the excess temperature, it is desirable to operate many engineering devices in the nucleate boiling regime. The approximate magnitude of the convection coefficient may be inferred by using Equation (2.1) with the boiling curve of Fig. 2.2.

2.3.3 Transition boiling

The region corresponding to $\Delta T_{e,C} \leq \Delta T_e \leq \Delta T_{e,D}$, is termed *transition boiling*, *unstable film boiling*, or *partial film boiling*. In this region bubble formation is so rapid that a vapor film or blanket begins to form on the surface. Because the thermal conductivity of the vapor is much less than that of the liquid, h (and q″) decreases with increasing ΔT_e.

2.3.4 Film boiling

When $\Delta T_e \geq \Delta T_{e,D}$, the region is termed as film boiling regime. At point D of the boiling curve, referred to as the *Leidenfrost point*, the heat flux is a minimum, q_{min} , and the surface is completely covered by a vapor blanket. Heat transfer from the surface to the liquid occurs by conduction and radiation through the vapor. As the surface temperature is increased, radiation through the vapor film becomes more significant and the heat flux increases with increasing wall superheat.

2.4 Nucleation

The life of a bubble can be summarized as occurring in the following phases: nucleation, initial growth, intermediate growth, exponential growth, asymptotic growth and possible collapse. *Nucleation* is a molecular-scale process in which a small bubble (nucleus) of a size just in excess of the thermodynamic equilibrium [Eq. (2.2)] is formed.

2.4.1 Equilibrium of a bubble

Assume that a spherical bubble of pure saturated steam is at equilibrium with superheated liquid. To determine the size of such a bubble, the conditions of mechanical and thermal

equilibrium is imposed. The bubble will be in mechanical equilibrium when the pressure difference between the inside and the outside of the bubble is balanced by the surface tension, σ, as indicated in the cutaway sketch in Fig. 2.4. Since thermal equilibrium requires that the temperature must be the same inside and outside the bubble, and since the vapor inside must be saturated at T_{sup} because it is in contact with its liquid, the force balance takes the form of *Young-Laplace equation*

$$R_b = \frac{2\sigma}{(p_{sat} at\ T_{sup}) - p_{ambient}} \tag{2.2}$$

The p-v diagram in Fig. 2.4 shows the state point of the internal vapor and external liquid for a bubble at equilibrium. Notice that the external liquid is superheated to ($T_{sup} - T_{sat}$) K above its boiling point at the ambient pressure; but the vapor inside, being held at just the right elevated pressure by surface tension, is just saturated. The equilibrium bubble whose diameter is described by Eq. (2.2) is unstable. If its radius is less than this value, vapor inside will condense and the bubble will collapse. If the bubble radius is slightly larger than the equation specifies, liquid at the interface will evaporate and the bubble will begin to grow.

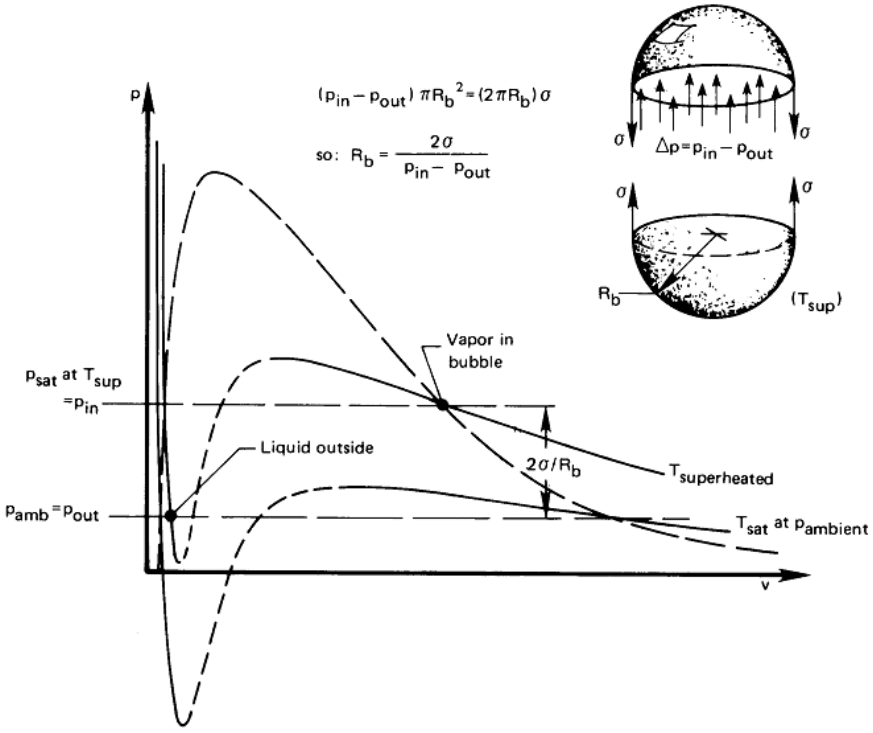

Fig. 2.4: Conditions for a bubble at equilibrium[19].

2.4.2 Superheated liquid

In nucleate boiling two separate processes - the formation of bubbles (nucleation) and the subsequent growth and motion of these bubbles were observed. In general, nucleation may be either of the homogeneous or heterogeneous variety; both types involve superheated liquid, which is a metastable state. The superheating of the liquid with respect to the saturation temperature that is required for nucleation to be achieved is referred to as the *nucleation superheat*. Eq. (2.2) with the help of *Clausius-Clapeyron equation* can be written as

$$R_b = \left(\frac{2\sigma}{H_{fg}\rho_g}\right)\left(\frac{T_{sat}}{T_g - T_{sat}}\right) \tag{2.3}$$

Where, $T_g = T_{sup}$. This expression gives the nucleation superheat ΔT_{nuc}, which is the difference between the saturation temperature of the vapor T_g at the pressure inside the nucleus p_g (= p_{in}) and the saturation temperature T_{sat} at the pressure in the surrounding liquid p_l (= p_{out}).

2.4.3 Homogeneous nucleation

Nucleation occurring in the bulk of a superheated, perfectly clear liquid is referred to as *homogeneous nucleation*. Some theories predict extremely high liquid superheats for nucleation in a pure liquid. Such high superheats are contrary to experimental observations of most engineering system.

In a real system the liquid contains foreign particles and dissolved gas that could act as nuclei. The predicted nucleation superheats would be considerably less in the presence of a preexisting gas phase. This form of homogeneous nucleation implies that vapor formation would be noted at random points where the nuclei happen to be located. In actual practice, however, bubbles form at specific locations associated with the heated surface, not the fluid. It has furthermore been found by microscopic observation that these locations are small imperfections or cavities on the heated surface [20].

2.4.4 Heterogeneous nucleation

Typical nucleation sites at the cavities or imperfection sites of heating surface are shown in Fig. 2.5. A large contact angle, Φ, may have a better chance to trap gas inside the cavity by a capillary effect. The wall superheat required for bubble growth to occur from a nucleation site of a solid surface was thought to be calculable from Eq. (2.3), where the critical radius may be taken as equal to the cavity radius. Such predictions, however, do not agree with observed data when a solid is used as the heating surface [21].

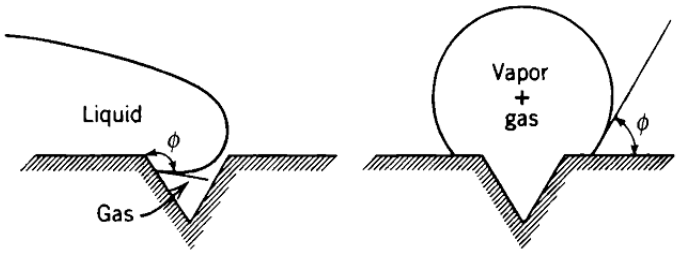

Fig. 2.5: Nucleation sites at the cavity.

Hsu [22] suggested that the criterion for the formation of a bubble on a solid surface, Eq.(2.3), is invalid when the solid surface alone is hot, and the difference must be related to the nature of the temperature field in the liquid immediately adjacent to the solid. The liquid temperature can be represented by the temperature profile in a thermal layer. Because of turbulence in the bulk of the liquid, the thermal layer cannot grow beyond a limiting thickness δ. If the liquid in the thermal layer is renewed by some disturbance, the temperature profile will reestablish itself by means of transient conduction and will ultimately grow into a linear profile as time approaches infinity. There is one range of cavity size for which the bubble temperature is lower than the liquid temperature at the bubble cap. This is the size range in which the bubble embryo will grow to make a cavity into an active site. The maximum and minimum sizes can be determined by solving the following two equations,

$$\frac{T_b - T}{T_w - T} = \frac{\delta - c_1 r}{\delta} \tag{2.4}$$

And,

$$T_b - T_{sat} = \frac{2\sigma T_{sat}}{C_2 r_c H_{fg} \rho_g} \tag{2.5}$$

Here, $T_b = T_g$, bubble temperature. The above nucleation criterion for boiling agrees with the experimental results of Clark et al. [20] and of Griffith and Wallis [23]. It was also verified qualitatively by Bergles and Rohsenow [24].

Shai [25] followed Bergles and Rohsenow's approach and calculated the nucleation superheat as

$$T_g - T_{sat} = \frac{T_g T_{sat}}{B} log_{10}\left(1 + \frac{2\sigma}{rp_{sat}}\right) \tag{2.6}$$

Where, B is the constant of *Antoine equation*. Several modified versions of nucleation criteria have since been advanced. An example is the model proposed by Lorenta et al. [26], which takes into account both the geometric shape of the cavity and the wettability of the surface (in terms of contact angle, Φ). Mizukami [27], Nishio [28], and more recently, Wang and Dhir [29], have proposed that the instability of vapor nuclei in a cavity determines the inception superheat.

2.5 Bubble Dynamics

Bubble dynamics includes the processes of bubble growth, bubble departure, and reformation of the thermal layer (which is termed as *waiting period*). In the following paragraphs, each one of these processes is described separately.

2.5.1 Bubble growth

Having nucleated a bubble, the next stage in the boiling process is the growth of that bubble as a result of vaporization of liquid at its interface.

Bubble growth in an extensive liquid pool

There are two schools of thought regarding bubble growth in a liquid pool:

1. *Inertia controlled growth*. In this point of view, the growth rate is limited by how rapidly the growing bubble can push back the surrounding liquid. The heat transfer to the interface

is very fast and is not a limiting factor. Inertia-controlled growth is typical of the early stages of bubble growth, particularly when the superheat is high. In this region, the growth process was analyzed by Rayleigh [30]; the radius of the bubble r (t) increases linearly with time according to the relationship

$$r(t) = \left[\frac{2}{3}\left\{\frac{T_l - T_{sat}(p_l)}{T_{sat}(p_l)}\right\}\frac{h_{fg}\rho_g}{\rho_l}\right]^{\frac{1}{2}} t \tag{2.7}$$

Where, T_l is the temperature of the liquid pool in which the bubble is growing, $T_{sat}\,(p_l)$ is the saturation temperature corresponding to the liquid pressure, h_{fg} is the latent heat of vaporization, and ρ_g and ρ_l are the vapor and liquid densities, respectively.

2. *Heat-transfer-controlled growth*. Here, the growth rate is limited by the transfer of heat between the bulk liquid and the interface where vaporization is occurring. This limiting case usually applies to the later stages of bubble growth when the liquid superheat near the interface has been largely depleted. For this region, the bubble size varies with the square root of time (Plesset and Zwick [31]) and is given by

$$r(t) = \frac{2\Delta T_{sat} k_l}{h_{fg}\rho_g}\left(\frac{3t}{\pi\alpha_l}\right)^{\frac{1}{2}} \tag{2.8}$$

where, k_l is the liquid phase thermal conductivity, ΔT_{sat} is the superheat, and α_l is the liquid phase thermal diffusivity.

Mikic et al. [32] suggest an equation covering both the inertia-controlled and heat-transfer-controlled regions. Miyatake et al. [33] have produced a new general equation for bubble growth that more accurately covers the whole range than does that of Mikic et al. [32].

Bubble Growth from a Surface. In practice, since heterogeneous rather than homogeneous nucleation is the norm in boiling, bubble growth occurs from a solid surface. An idealized representation of the process is shown in Fig. 2.6. The following stages are identified:

1. At t = 0, the previous bubble has just departed from the surface, carrying with it the thermal boundary layer. The bulk fluid (at temperature T_∞) is brought into contact with the wall and the thermal boundary layer begins to grow again by transient conduction from the heated surface.

2. During a waiting period t_w, no significant growth of the bubble occurs. During this period, the thermal boundary layer is building up on the surface and it is only after the period t_w that bubble growth can commence.

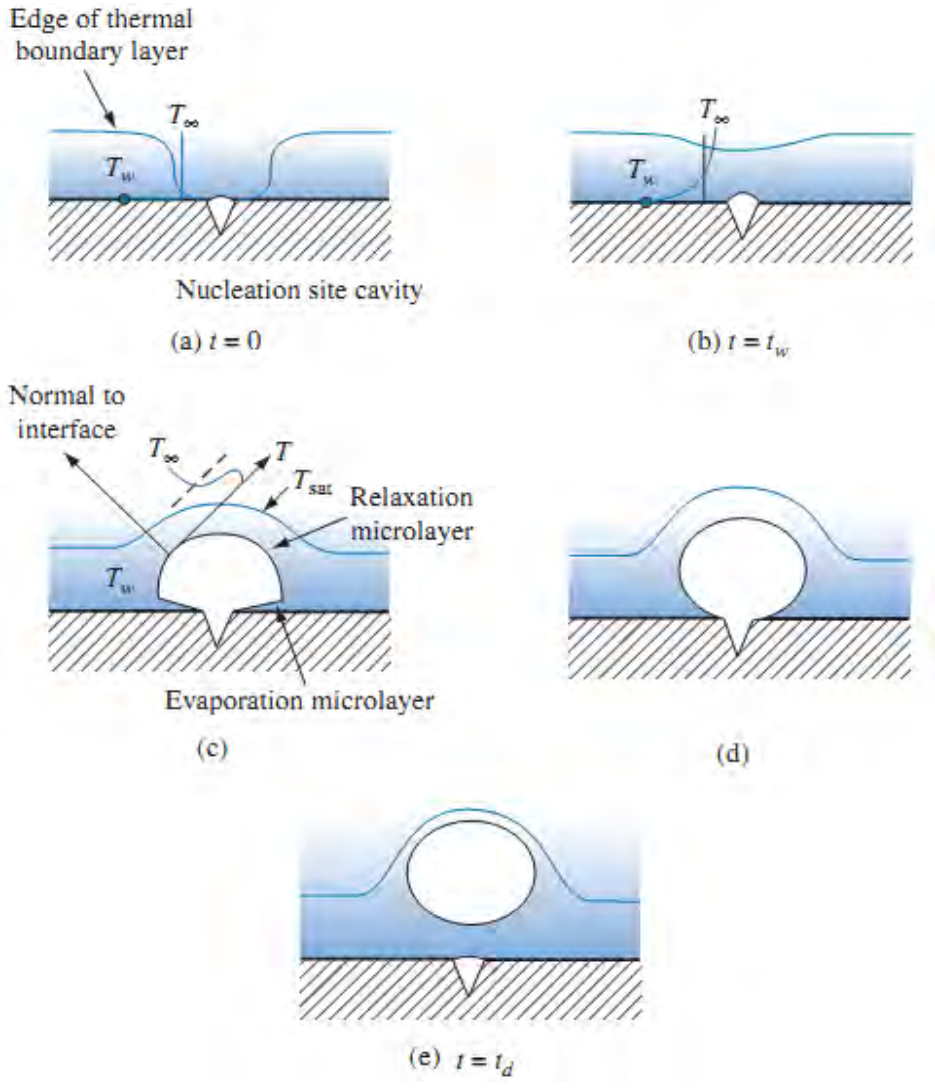

Fig. 2.6: Stages in a bubble growth from a cavity in a heated surface[12]

3. Once the waiting period is over, rapid inertia-controlled bubble growth occurs, the bubble growing in a nearly hemispherical shape as shown in Fig. 2.6c. In this period, a liquid microlayer may be left behind that has a thickness near zero at the original nucleation site (evaporation microlayer) and a finite thickness at the edge of the hemispherical bubble (relaxation microlayer). The bubble grows as a result of both evaporation at its upper surface (which is in contact with superheated liquid in the displaced boundary layer) and also by evaporation of this microlayer.

4. After the initial rapid growth stage, the growth rate decreases and the bubble growth may become heat-transfer-controlled rather than inertia-controlled; this results in a more spherical bubble as shown in Fig. 2.6d.

5. The bubble is released from the surface at the departure time t_d. The released bubble carries with it a portion of the thermal boundary layer and the cycle is repeated.

2.5.2 Bubble departure and bubble departure frequency

In nucleate boiling bubble departure is another fundamental process of importance. The diameter at which a bubble departs from the surface during its growth is controlled by buoyancy and inertia forces (each attempting to detach the bubble from the surface) and surface tension and hydrodynamic drag forces (both resisting its departure). Furthermore, the shape of the bubble may deviate significantly from the idealized spherical shape. While slowly growing bubbles tend to remain spherical, rapidly growing bubbles tend to be hemispherical. Numerous other shapes are observed using high-speed movie cameras or videos [34]. The bubble departure frequency is expressed by the following equation

$$f = \frac{1}{t_g + t_w} \tag{2.9}$$

where, t_g is the bubble growth time and t_w is the waiting time between the departure of one bubble and the initiation of growth of the next. Bubble departure frequencies range from as low as 1 Hz at very small superheats to over 100 Hz at high superheats. The bubble growth

time t_g can be obtained by calculating the bubble departure diameter in extended Fritz equation [34] and solving for time t in the Plesset–Zwick bubble growth equation presented earlier in Eq. (2.8). After a bubble departs, the length of pause before the next bubble begins to grow depends on the rate at which the surface and adjacent liquid are reheated by transient heat conduction from the wall.

2.6 Nucleate Boiling Heat Transfer Mechanism

In Fig. 2.7 nucleate pool boiling heat transfer mechanisms are illustrated. Several suggested models of heat transfer mechanisms are depicted below:

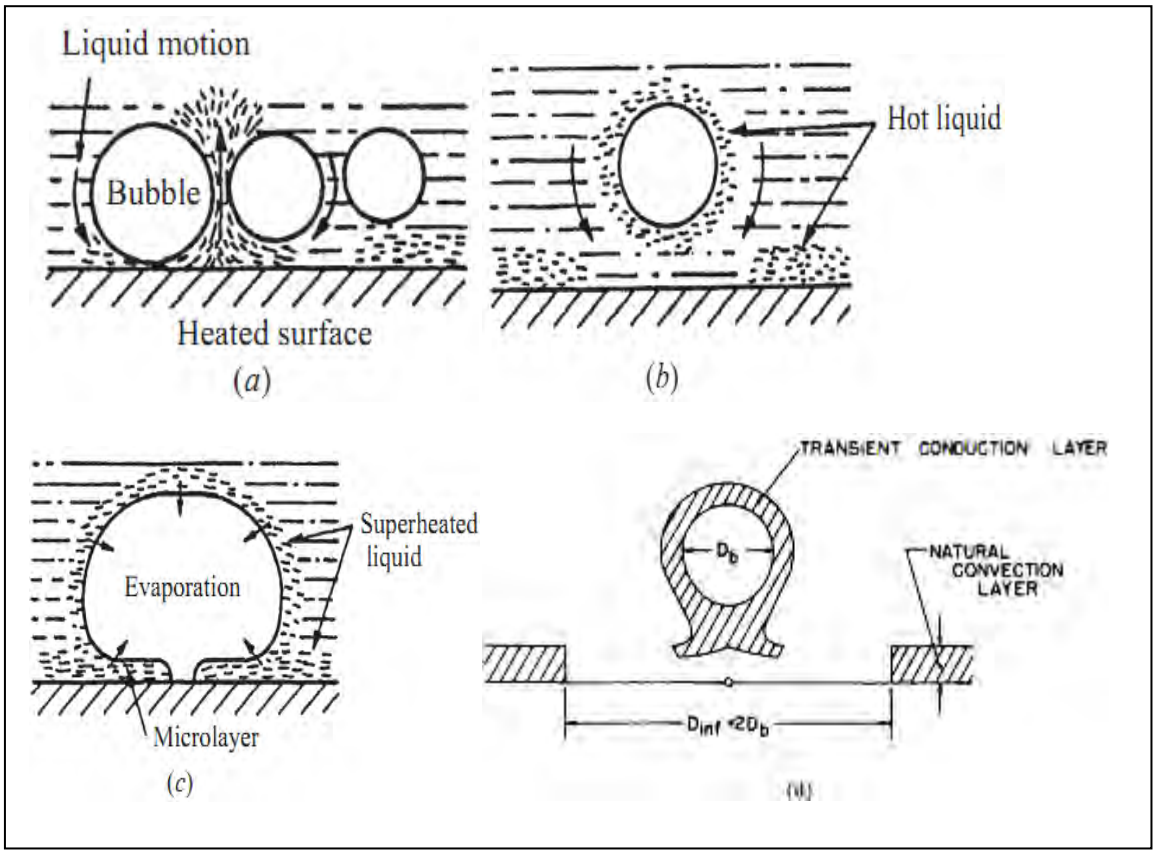

Fig. 2.7: Heat Transfer mechanism in nucleate pool boiling: (a) bubble agitation, (b) vapor-liquid exchange, (c) evaporation, and (d) transient conduction to, and subsequent replacement of, superheated liquid layer.

Bubble agitation. The systematic pumping motion of the growing and departing bubbles agitates the liquid, pushing it back and forth across the heater surface, which in effect transforms the otherwise natural convection process into a localized forced convection process. Sensible heat is transported away in the form of superheated liquid and depends on the intensity of the boiling process. An appreciable degree of fluid mixing occurs near the heater surface during boiling [35]. While this mechanism can be an important contributor to the effective nucleate boiling coefficient, it does not appear to be a singular cause of the large heat transfer coefficient noted in nucleate boiling [36].

Vapor–liquid exchange. This model [18] is in some respects similar to the bubble agitation model, but it avoids certain objections of the latter. The wakes of departing bubbles remove the thermal boundary layer from the heated surface, and this creates a cyclic thermal boundary layer stripping process. Sensible heat is transported away in the form of superheated liquid, whose rate of removal is proportional to the thickness of the layer, its mean temperature, the area of the boundary layer removed by a departing bubble, the bubble departure frequency, and the density of active boiling sites.

Evaporation. Heat is conducted into the thermal boundary layer and then to the bubble interface, where it is converted to latent heat. Macro-evaporation occurs over the top of the bubble while micro-evaporation occurs underneath the bubble across the thin liquid layer trapped between the bubble and the surface, the latter often referred to as microlayer evaporation. The rate of latent heat transport depends on the volumetric flow of vapor away from the surface per unit area.

Transient conduction to, and subsequent replacement of, superheated liquid layer. This mechanism is shown in Fig. 2.7d. Mikic and Rohsenow considered this model [37], which was first suggested by Han and Griffith [38], to be the single most important contributor to the heat transfer in nucleate boiling. Based on an implicit reasoning, they disregarded the evaporation of the microlayer as a dominant factor in most practical cases. With the basic mechanism for a single active cavity site, a departing bubble from the heated surface will remove with it (by action of a vortex ring created in its wake) a part of the superheated layer. The area from which the superheated layer is removed,

known as the area of influence, can be approximately related to the bubble diameter at departure as [38] (Fig. 2.7d)

$$D_{inf} = 2D_b \tag{2.10}$$

Following the departure of the bubble and the superheated layer from the area of influence, the liquid at T_{sat} from the main body of the fluid comes in contact with the heating surface at T_w. This bears some similarity to the vapor-liquid exchange mechanism, except for the quantity of liquid involved.

The mechanisms described above compete for the same heat in the liquid and hence overlap with one another. At low heat fluxes characteristic of the isolated bubble region, natural convection also occurs on inactive areas of the surface, where no bubbles are growing.

2.7 Correlations

Boiling at a heated surface is a very complicated process, and it is consequently not possible to write and solve the usual differential equations of motion and energy with their appropriate boundary conditions. No adequate description of the fluid dynamics and thermal processes that occur during such a process is available, and more than two mechanisms are responsible for the high heat flux in nucleate pool boiling. Over the years, therefore, theoretical analyses have been for the most part empirical, and have leaned on the group parameter approach. Since the high liquid turbulence in the vicinity of the heating surface is considered to be dominant, at least in a portion of the ebullition cycle, it is natural to correlate the boiling heat transfer rates in a similar fashion as in single-phase turbulent-flow heat transfer phenomena by an equation of the type

$$Nu = f(Re, \mathrm{Pr})$$

Thus many theoretical correlations start with the form

$$Nu_b = a(Re_b)^m, (\mathrm{Pr_l})^n \tag{2.11}$$

Where, a = a constant coefficient

m, n = constant exponents

Nu_b = boiling Nusselt number

Pr_l= liquid Prandtl number

Rohsenow's early correlation. Using the form of correlation shown in Eq. (2.11), and assuming that the bubble agitation mechanism depicted in Fig. 2.7(a) is of prime importance, Rohsenow found empirically [39], with data obtained from a 0.024-in. (0.6-mm) platinum wire in degassed distilled water, that

$$\frac{c_l(T_w - T_{sat})}{H_{fg}} = c_{sf}\left[\frac{q}{{}_lH_{fg}}\sqrt{\frac{g_c\sigma}{g(\rho_l - \rho_g)}}\right]^n \left(\frac{c_l{}_l}{k_l}\right)^{m+1} \qquad (2.12)$$

This equation was shown to correlate well not only with boiling data for water in a pressure range of 0.l to 16.8 MPa, but also with other data of different surface. This equation gives $\Delta T \propto q^{\ n}$ and h is obtainable from its definition (i.e., h =q″/ΔT, where $\Delta T = T_w - T_{sat}$ and T_w is the wall temperature). The exponents are m =0.7 and n =0.33 (thus equivalent to $q'' \propto \Delta T^3$), except for water, where m =0. Physical properties are evaluated at the saturation temperature of the fluid.

The most important variables affecting C_{sf} are the surface roughness of the heater, which determines the number of nucleation sites at a given temperature [40], and the angle of contact between the bubble and the heating surface, which is a measure of the wettability of a surface with a particular fluid. A totally wetted surface has the smallest area covered by vapor at a given excess temperature and consequently represents the most favorable condition for efficient heat transfer. In the absence of quantitative information on the effect of wettability and surface conditions on the constant C_{sf}, its value must be determined empirically for each fluid-surface combination. Rohsenow provided a list of values of C_{sf} for various surface–fluid combinations. Values of C_{sf} is listed in Table A.1. Because this method requires a surface–fluid factor, it is not convenient to use for general thermal design.

Reduced Pressure Correlation of Cooper with Surface Roughness Cooper proposed the following reduced pressure expression for the nucleate pool boiling heat transfer coefficient [41]:

$$h = 55{p_r}^{0.12-0.4343lnR_p}(-log_{10}p_r)^{-0.55}M^{-0.5}q^{0.67} \tag{2.13}$$

Note that this is a dimensional correlation in which h is in W/m^2 ·K, the heat flux q is in W/m^2, and M is the molecular weight and R_p the mean surface roughness in micrometers (R_p is set to 1.0 μm for undefined surfaces). Increasing the surface roughness has the effect of increasing the nucleate boiling heat transfer coefficient.

Fluid-Specific Correlation of Gorenflo. Gorenflo proposed a reduced pressure type of correlation that utilizes a fluid-specific heat transfer coefficient α_0 defined for each fluid at the fixed reference conditions of p_{r0} =0.1, R_{p0} =0.4 μm, and q_0 = 20,000 W/m^2 [42]. His values for α_0 are given in Table A.3 for various fluids. The general expression for the nucleate boiling heat transfer coefficient α_{nb} at other conditions is

$$\alpha_{nb} = \alpha_0 F_{PF}\left(\frac{q}{q_0}\right)^n\left(\frac{R_p}{R_{p0}}\right)^{0.133} \tag{2.14}$$

Where, the pressure correction factor F_{PF} is

$$F_{PF} = 1.2{p_r}^{0.27} + 2.5p_r + \frac{p_r}{1-p_r} \tag{2.15}$$

And, p_r is the reduced pressure. The exponent n on the heat flux ratio is also a function of reduced pressure:

$$n = 0.9 - 0.3{p_r}^{0.3} \tag{2.16}$$

This method is accurate over a very wide range of heat flux and pressure and is probably the most reliable of those presented [34].

2.8 Enhancement Techniques in Pool Boiling

Study of the boiling heat transfer enhancement is one of the fastest growing areas of research in recent years. In many cases, for the following two reasons enhancement techniques of boiling heat transfer are employed

- To decrease the temperature difference between the heat transferring media for realizing the higher thermal cycle performance at the constant volume of heat exchangers.
- To increase the heat flux at a constant temperature difference for realizing compact heat exchangers with higher heat transfer coefficients and smaller surface area.

An exhaustive compilation of the literature related to enhancement techniques of heat transfer has been presented by Bergles [3,43,44,45], Webb and Bergles [46], Bergles et al. [2], Thome [47], Webb and Kim [48].

Bergles has identified fourteen different heat transfer enhancement techniques [44]. He classified these techniques as (i) *passive techniques*, (ii) *active techniques* and, (iii) *compound techniques*. Compound heat transfer enhancement technology combines at least two heat transfer enhancement methods.

2.8.1 Active techniques

Active techniques require an activator/power supply to bring about the enhancement. Examples of active techniques are *surface wiping-rotation*, the use of *electro-hydrodynamic (EHD) enhancement* and the use of *ultrasound fields*. In EHD enhancement, a high voltage (typically 5-25 kV) is applied to the boiling surface and this produces electrically induced secondary motions that can give a very high enhancement in boiling heat transfer. Examples of investigations in this area are those of Ohadi et al. [49], and Zaghdoudi et al. [50]. EHD has obvious safety implications, but by adjusting the surface voltage, it is possible to control the heat transfer rate, and this may be useful in some applications. Boiling in ultrasound fields has been studied by Bonekamp and Bier [51]; they show that significant improvements in boiling heat

transfer can be obtained using ultrasound fields, particularly in the case of mixture boiling. Ultrasound fields also diminish the tendency toward the hysteresis effect.

2.8.2 Passive techniques

Of the available heat transfer enhancement technology, passive heat transfer enhancement technology is of more practical use and is easily implemented because it does not consume external power. Various passive heat transfer enhancement methods have been developed over the past years, for example, *rough surface*, *structured surface*, *finned tubes*, *additives for fluids* and so on. Structured *enhancement surfaces* are used commercially for augmentation of nucleate boiling. Enhancement surfaces are of two types: (1) coatings of very porous material formed by sintering, brazing, flame spraying, electrolytic deposition, or foaming, and (2) mechanically machined or formed double-reentrant cavities to ensure continuous vapor trapping. Such surfaces provide for continuous renewal of vapor at the nucleation sites and heat transfer augmentation by more than an order of magnitude.

2.9 Enhancement with Surfactant

Among the different nucleate boiling heat transfer enhancement techniques, the use of additives such as surfactants and polymeric additives for liquids, as a passive technique, appears to be quite viable and has attracted much more research interests over the past decades [52]. The study of boiling phenomena with surfactants and polymeric additives may go back to a very earlier research of flow boiling with surfactants by Stroebe et al. in 1939 [53] and an earlier research of pool boiling with surfactants by Morgan et al. in 1949 [54]. After these, a lot of research of boiling phenomena with surfactants and polymeric additives has been conducted. It is a very active research topic at present. Small amounts of certain surfactants in water have been known to enhance the rate of nucleate pool boiling heat transfer of water significantly [4,5,6,7,55,56,57].

Because of their low concentration, the presence of surfactants in water causes no significant change in the solvent physical properties except for surface tension, whereas the presence of polymers or surfactants at higher concentrations in water may causes big change of the viscosity in the solvent (non-Newtonian fluidic behavior).

Frost and Kippenhan [58] investigated boiling of water with varying concentrations of surfactant “Ultra Wet 60L”. They found an increase in heat transfer and concluded that it resulted from the reduced surface tension. Heat transfer in nucleate pool boiling of dilute aqueous polymer solutions was measured by Kotchaphakdee and Williams [59] and compared with results for pure water. Photographs showed distinct differences in bubble size and dynamics, between polymeric and non-polymeric liquids. Gannett and Williams [60] concluded that surface tension was not relevant in explaining the enhancement effect, and reported that viscosity could be a generally successful correlating parameter.

Yang and Maa [4] studied pool boiling of dilute surfactant solutions. The surfactants used in this study were sodium lauryl benzene sulfonate and sodium dodecyl sulfate (SDS). Since all experiments were carried out under very low concentrations, it was concluded that these additives had no notable influence over the physical properties of the boiling liquid, except surface tension, which was significantly reduced. This study showed that the surface tension of the boiling liquid had significant influence on the boiling heat transfer coefficient.

Pool boiling experiments were carried out by Tzan and Yang [5], for relatively wide ranges of surfactant concentration and heat fluxes. The results verify again that a small amount of surface-active additive makes the nucleate boiling heat transfer coefficient of water considerably higher. It was also found that there is an optimum additive concentration for highest heat flux. Beyond this optimum point, further increase in the concentration of the additive lowers the boiling heat transfer coefficient. Experimental data on the effect of surfactants on nucleate boiling heat transfer in water with nine additives were reported by Wu et al. [61] . Anionic, cationic, and non-ionic surfactants were studied at concentration up to 400 ppm (parts per million). The enhancement of heat transfer was related to the depression of static surface tension.

Hetsroni et al. [57] demonstrate that the heat transfer coefficient of the boiling process can be enhanced considerably by the addition of a small amount of Habon G. The heat transfer increases at low surfactant concentration, reaches a maximum and decreases with further increase in concentration. The effect of both the surface tension and the kinematic viscosity

of surfactant mixture can explain the features of heat transfer at boiling of surfactant solutions.

Wen and Wang [62] experimented with SDS and Triton X-100 and concluded that the wettability is an important parameter in surfactant boiling and should be taken into consideration. He also concluded that neither kinematic viscosity nor surface tension theory alone could give a persuasive explanation in surfactant boiling.

A state-of-the-art review on the current status of pool boiling research with surfactant additives is presented by Cheng et al. [10].

Boiling phenomena with surfactants

Boiling with surfactant additive is generally an exceedingly complex process, and it is influenced by a larger set of variables than the phase-change process of pure water. Besides the wall superheat, heating surface geometry, and bulk concentration of additives, the nucleate boiling behavior is also dependent upon, among others, the role played by interfacial properties (surface tension and contact angle), the nucleate process, Marangoni effects and foaming. It appears that the boiling mechanism itself is influenced by the nature of additive and its chemistry in the solution [52].

It was recognized long time ago that surface tension plays an important role in boiling process. Considering the role of surface tension in boiling heat transfer, Westwater [63] assumed the following heat transfer coefficient relationship with surface tension

$$h \propto \sigma^n \tag{2.17}$$

As pointed out by Lowery and Westwater [64], earlier literature is contradictory about the role of surface tension during boiling process. Some researchers have reported that surface active agents in water increase heat transfer at a given temperature difference driving force, while others have reported a decrease. A dozen values have been published for the exponent n, which has values ranging from -2.5 to +1.275 [64]. Apparently it is contradictory for the role of surface tension in the boiling process. With negative exponent values, the reduction in surface tension increases boiling heat transfer coefficient whereas

with positive exponent values, the reduction in surface tension decreases boiling heat transfer coefficient. However, theoretically surface tension is an important variable in boiling process. Rate of formation of vapor nuclei in the boiling of a liquid is proportional to surface tension as [63]:

$$n \propto e^{-\sigma^3} \tag{2.18}$$

Thus, small decrease in surface tension should causes large increase in the number of nuclei. This has been confirmed by the visualization of nucleate boiling process conducted by a lot of researchers. For example, Zhang [65] observed the nucleate boiling process by means of a high-speed camera and compared the observed results for water and surfactant solutions. His observation has firmly confirmed this point. In addition, cavitation theory predicts that force required to rupture a liquid in tension is proportional to surface tension as[63]:

$$F \propto \sigma^{\frac{3}{2}} \tag{2.19}$$

Thus, liquids with large surface tensions should be difficult to fracture.

The nucleate pool boiling heat transfer has generally been observed to increase with increasing the concentration of aqueous surfactant solutions. However, when the solution concentration is larger than *critical micelle concentration* (cmc), there will be reduction in boiling heat transfer enhancement [10].

2.10 Surfactant

The name surface-active agent and surfactant is interchangeably used which means a compound is active at surface. Surface active substances or surfactants are amphiphilic compounds having a lyophilic, in particular hydrophilic part (polar group) and a lyophobic, in particular hydrophobic part (often hydrocarbon chain) [see Fig. 2.8]. The amphiphilic structure of surfactants is responsible for their tendency to concentrate at interfaces and to aggregate in solutions into various supramolecular structures, such as micelles and bilayers.

According to the nature of the polar group, surfactants can be classified into nonionic and ionic surfactants, which may be of anionic, cationic, and amphoteric or zwitterionic nature. Nonionic surfactants have no charge, anionic surfactants have a negative molecular charge, cationic surfactants have a positive molecule charge, and amphoteric or zwitterrionic surfactants have both positive and negative charges [66,67]. Anionic and nonionic surfactants provide most of industrial surfactant requirements and are the most common.

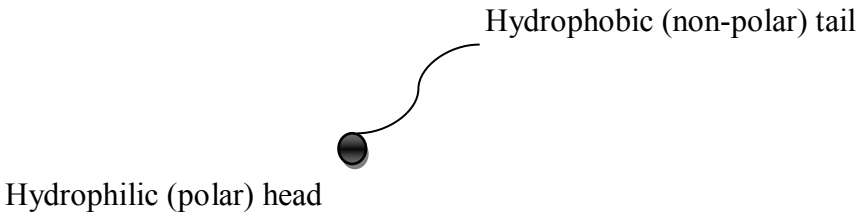

Fig. 2.8: Schematic illustration of primary structure of a surfactant.

They have a natural tendency to adsorb at the liquid-vapor interface with their polar head oriented towards the aqueous solution and the hydrocarbon tail directed towards the vapor.

2.10.1 Colloid systems and interfacial phenomena

When a state of matter is finely dispersed in another, then a colloidal system is obtained. Colloidal systems often exhibit rather unusual phenomena at their phase boundaries (interfaces), relative to the expected bulk phase interactions, such that the behavior of the entire system is controlled by interfacial processes [68,69]. Interfacial phenomena are important in Boiling. With nucleate phase-change and ebullience in aqueous surfactant solutions, which are association colloid systems, where molecules of surface-active substances (e.g. surfactants) are associated together to form small aggregates (micelles) in water, the aggregates formed may often adopt an ordered structure. The consequent interfacial changes significantly affect boiling.

Altogether five different interfaces can exist: gas-liquid, gas-solid, solid-liquid, liquid-liquid, and solid-solid. In the case of surfactant solutions, the additive may adsorb at all of the five types of interfaces. For nucleate pool boiling in aqueous surfactant solutions, however, there are two primary interfaces that have a dominating influence: (1) vapor-liquid interface, at which the surface tension reduces because of the surfactant adsorption-

desorption process, and (2) solid-liquid (or heater-liquid) interface, where the surfactant physisorption occurs and the surface wetting behavior changes.

2.10.2 Surface tension

Surfactants greatly reduce the surface tension of solvents, water and water-based solutions, inks, fountain solutions, adhesives and other coating formulations. To reduce the surface tension, however, surfactant molecules have to migrate to the interface, and this takes some finite amount of time. The formulation will eventually reach *equilibrium (static) surface tension* after certain time. This takes several seconds or even several hours depending on the type of surfactant and the concentration of solutions. During this dynamic process before reaching equilibrium, the surface tension changes with the time and thus is defined as *dynamic surface tension*. In general, surfactants with smaller (lighter) molecule mass (short hydrophobic tail) diffuse more rapidly to the interface than that with larger (higher) molecule mass. Higher molecular weight surfactants affect a higher equilibrium surface-tension depression compared to lower molecular weight surfactants [67].

In addition, most surfactants at higher concentrations cause change of the physical properties of the surfactant solutions and cause strong surface films between adjacent molecules, the strength of which determines surface properties of the surfactant solutions. In general, surface tension decreases with increasing surfactant solution concentration, and dynamic surface tension is usually higher than equilibrium surface tension at a fixed concentration. Higher solution temperature results in lower surface tension in both equilibrium and dynamics conditions. Additionally for all surfactants, surface tension decreases asymptotically with increasing concentration. The asymptotic limit is commonly referred to as the *critical micelle concentration* (cmc) of the surfactants. Critical micelle concentration (cmc) is characterized by micelle formation, or *micellization*, which is the property of surface-active solutes that lends to the formation of colloid-sized clusters, i.e. at a particular concentration, additives form aggregates in the bulk phase or a surfactant cluster in solution that are termed micelles. Different shapes and sizes of micelles such as globular or spherical, rod-shaped or cylindrical, and lamellar or plate-like exist depending

upon the surfactant type and its concentration, solution temperature, presence of other ions and water-soluble organic compounds in the solutions. The micelle is a dynamic entity and its structure and shape can change with time. Critical micelle concentration (cmc) may be determined by many different techniques. A survey of methods for cmc determination is summarized by Lange [66]. Popular techniques include surface tension, turbidity, self-diffusion, conductivity, osmotic pressure, solubilization, surfactant selective electrodes and fluorescence methods. Nearly all of these methods involve plotting a measurement as a function of surfactant concentration or as a function of the logarithm of surfactant concentration. The cmc is then deduced as a breakpoint. Critical micelle concentration is an important parameter in boiling phenomena with surfactants.

Fig. 2.9 shows the variation of the measured equilibrium surface tension versus the solution concentration which was measured by Wu et al. [61]. It can be concluded that surface tensions decrease with increasing additive concentrations for all the nine surfactants.

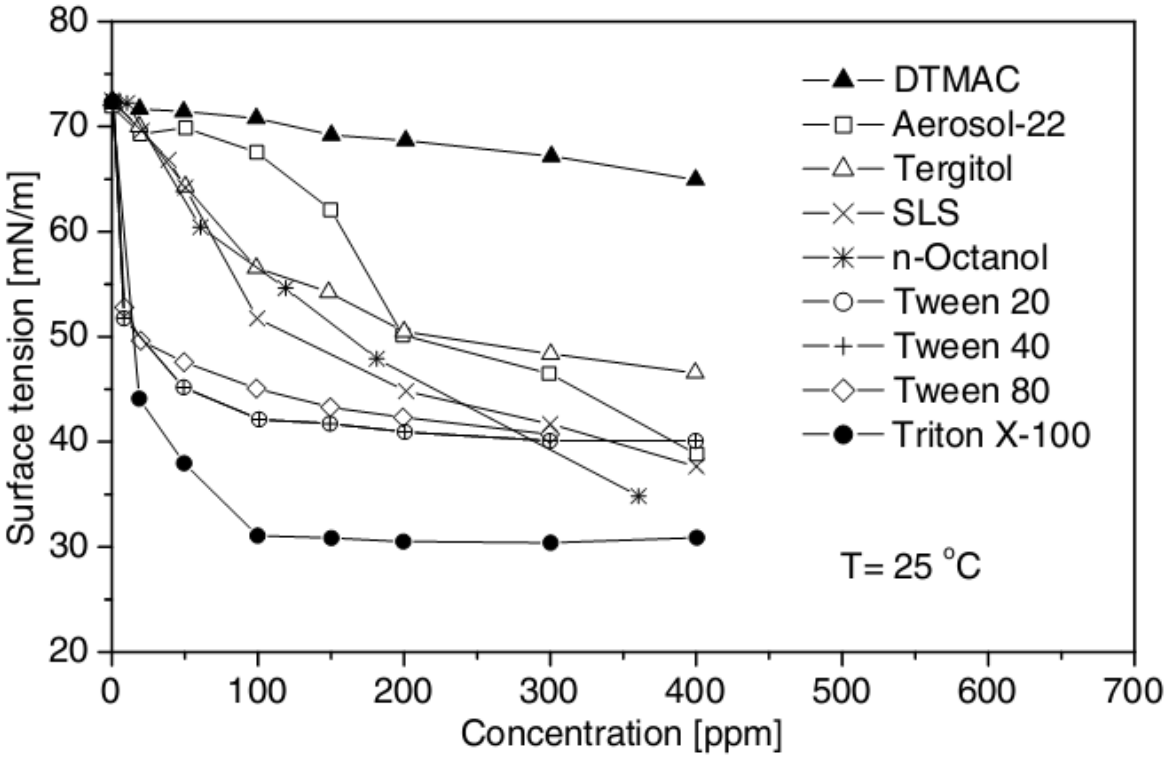

Fig. 2.9: Variation of the measured equilibrium surface tension versus concentration presented by Wu et al. [61].

3. EXPERIMENTAL

Experimental works include: a) construction of a set-up for studying saturated nucleate pool boiling heat transfer, b) measurements of change of heat flux with wall superheat for water and water with sodium oleate additive, c) measurements of surface tension of sodium oleate solution, and d) measurements of surface roughness of the heater surface.

3.1 Experimental Setup

A schematic diagram of the experimental setup used in the pool boiling study is shown in Fig. 3.1. A cartridge type electric heater is placed horizontally in a glass column. The heater surface is illuminated, and is photographed from outside of the glass column. The non-heated part of the heater is placed in a Teflon rod. This placement reduced strain on the lead wire. The cartridge heater is made of a seamless stainless steel tube having 1.27 cm outer diameter and 12.5 cm length. The 220 V, 1400 W heater provided a peak heat flux of about 335 kW/m^2. The junction of the thermocouple is placed at the central position of the sheath's internal surface. The wall surface temperature is measured with this thermocouple-digital readout meter. As the heater is sufficiently long and thin, the heat conduction in the axial direction can be neglected.

The pool temperature is measured by a calibrated thermocouple-digital readout meter. A mercury manometer is used to monitor the pool pressure throughout the experiment. A coiled-tube water-cooled condenser is provided for condensing the generated vapor and returning the condensed liquid into the pool. Rate of water flow through the condenser is controlled by manual valve to maintain atmospheric pressure in the pool. As the amount of subcooled returned condensate is very small in comparison to the amount of saturated liquid in the vessel, the return of the liquid condensate has no or little effect on the pool liquid temperature.

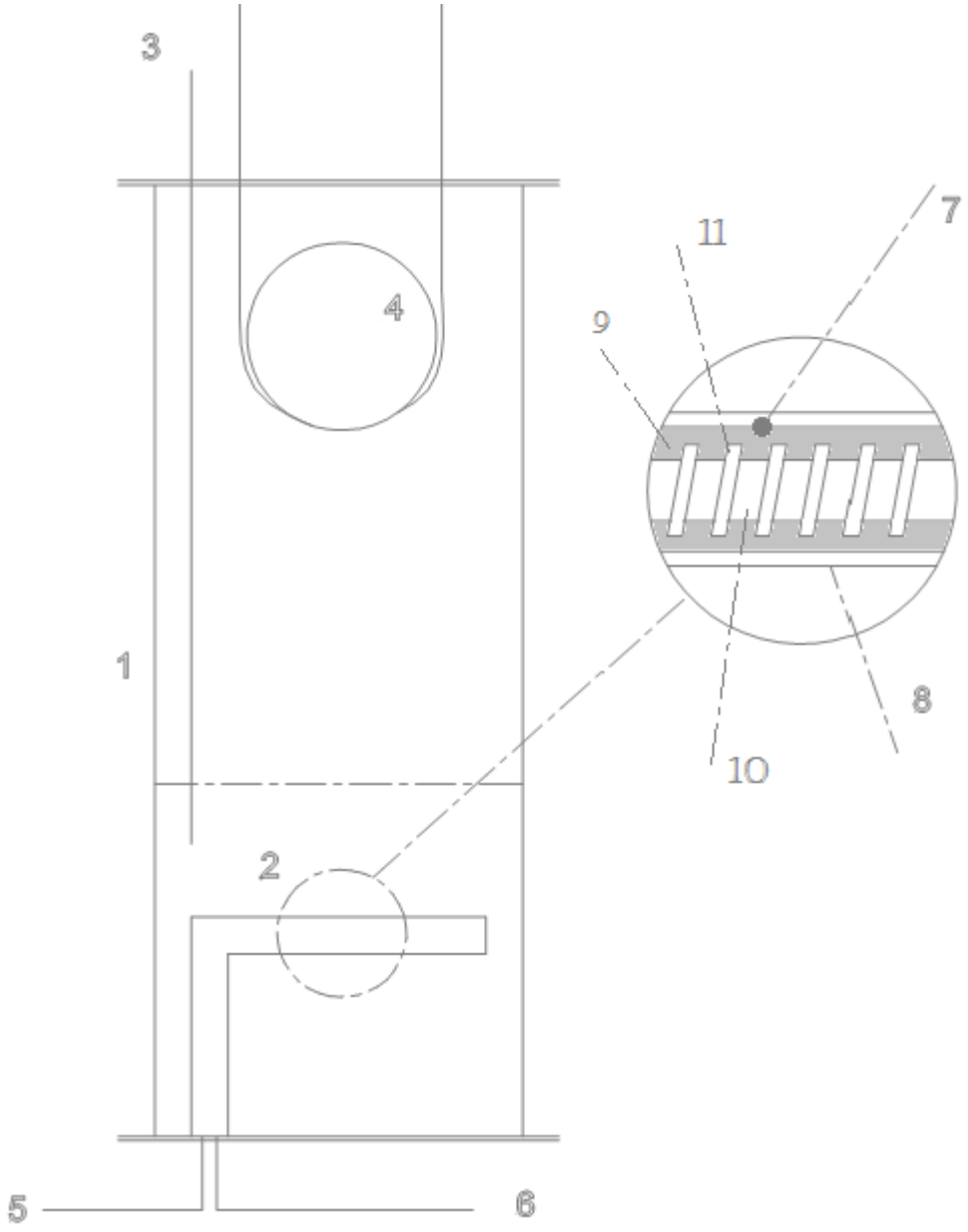

Fig. 3.1: Schematic of pool boiling apparatus: (1) glass column vessel; (2) heating element with provision for surface temperature measurement; (3) temperature probe for bulk fluid temperature measurement; (4) water-cooled condenser coil; (5) thermocouple to digital meter; (6) AC power supply; (7) thermocouple junction; (8) stainless steel tube; (9) insulation powder; (10) ceramic core; (11) heating coil.

A variac-controlled AC power supply, a panel voltmeter, a clamp meter, and an electricity meter provided the necessary controls and measurements of the input electric power during the experiment. An image of the experimental setup is given in Fig. 3.2.

Fig. 3.2: An image of the experimental setup.

3.2 Main Components of the Experimental Setup

The main components of the experimental setup with their specifications are described below:

Heater

The cartridge heater is made of a seamless stainless steel tube having 1.27 cm outer diameter and 12.5 cm length. The 220 V, 1400 W heater is supplied by *Rotterdamse Elementen Fabriek* of Netherlands. It provided a peak heat flux of about 335 kW/m^2. A k type thermocouple is internally grounded to the sheath's surface. The specification sheet of the heater is given in Fig. 3.3. Optical microscope images of the roughness characteristics of heater surface is captured and showed in Fig. 3.4. This image clearly shows a random distribution of pits, cavities and machining grooves of varying shapes and sizes along the heater surface.

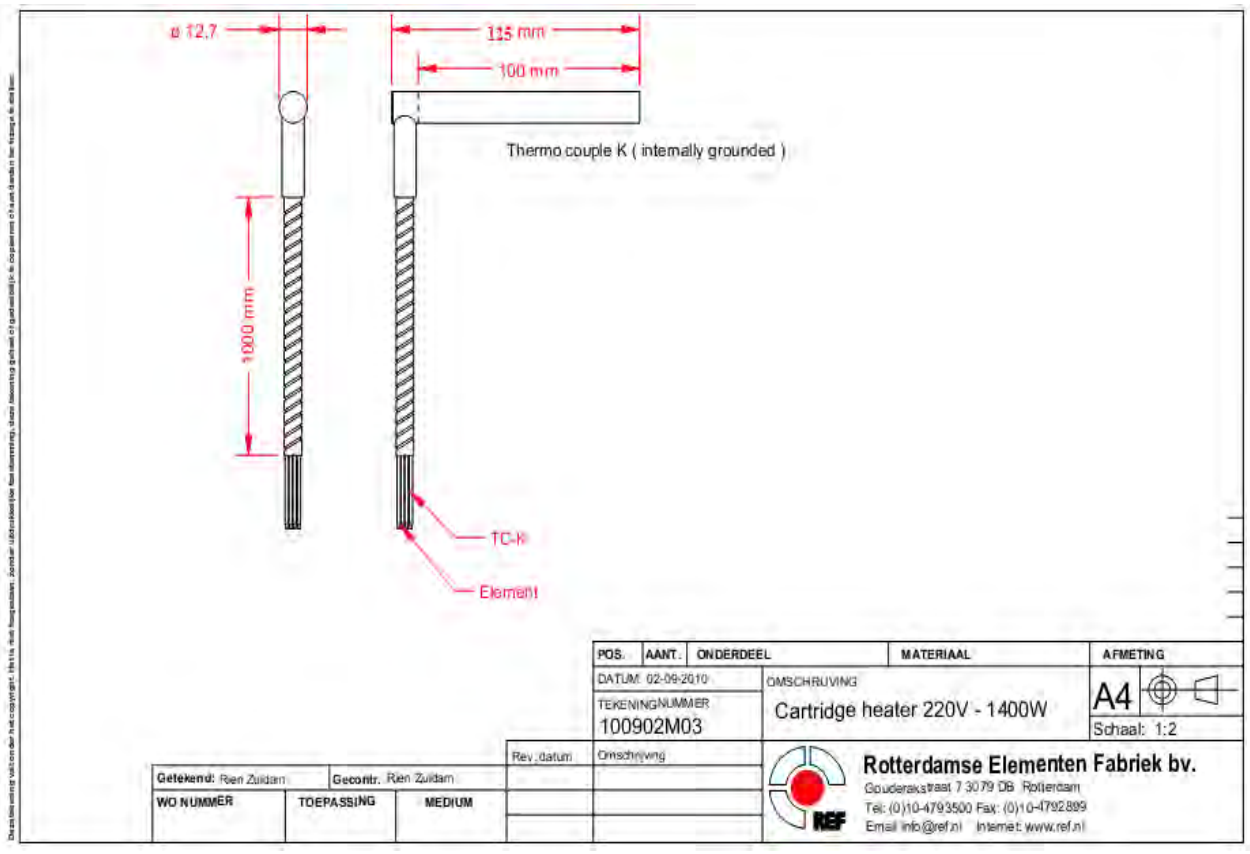

Fig. 3.3: Specification of the custom made cartridge type electric heater.

100X

200X

Fig. 3.4: Optical microscope images of the roughness characteristics of heater surface.

Glass column

A glass column having 17.8 cm outer diameter and 40.6 cm height is used in this setup. The diameter of the glass column is dictated by the heater length. This glass column housed the electric heater and allowed to photograph the nucleate boiling. The height of the column is set by three factors: the height of the test fluid, the degree of foaming that might occur from heating of water with surfactant experiments and the height of the condenser system fitted at the top of the column.

3.3 Experimental Procedure

Deionized water is used for all the experimental works. Distilled water is passed through a resin bed to get the deionized water. Properties of deionized water are given in Table 3.1. The boiling curve for water is established over two month's period to check the repeatability and aging effect of the heater. For each boiling test run, the column is loaded with 2000 ml of liquid to bring the liquid surface to a level of 60 mm above the heater surface. In this study power-controlled method of heating is used. After achieving the liquid saturation temperature, the test is carried out by varying the wall heat flux in a stepwise manner. Heat flux is varied both in increasing and decreasing order, and no significant change is noticed. Surfactant solutions are replaced by deionized water in between two test runs. This precaution validates the experimental reliability of the apparatus.

Table 3.1: Properties of deionized water at 28°C.

Conductivity, mS/cm	0.001
Surface tension, mN/m	71.7
pH	7.08

Different concentration of sodium oleate solutions are prepared by weighing a definite amount of the sodium oleate powder with a sensitive digital balance and adding it to the deionized water.

An electric meter is used for measuring the power input of the heater. Voltage across and current through the heater is also measured. From the measured power input and effective heat transfer area of the heater, heat flux is calculated. A sample calculation is shown in Appendix B. Temperature reading of the heater surface and the pool liquid are measured with the calibrated digital readout meter and k type thermocouple combination.

3.4 Sodium Oleate

The sodium salt of Oleic acid (cis-9-octadecenoic acid) is supplied by BDH Laboratory Supplies, UK. This anionic surfactant is a component of commercial soaps and is soluble in water.

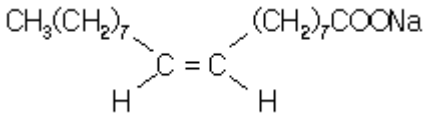

Fig. 3.5: Structure of sodium oleate.

The physico-chemical properties of the surfactant powder are listed in Table 3.2. The structure of sodium oleate is shown in Fig. 3.5.

Table 3.2: Physico-chemical properties of Sodium Oleate.

Chemical formula	$C_{18}H_{33}NaO_2$
Ionic type	anionic
Appearance	Brownish-white
Molecular weight	304
Water solubility	100g/l (100,000 ppm)

3.5 Surface Roughness Measurement of the Heater

As the surface roughness of the heater surface significantly influences the boiling characteristics, it is measured with Surtronic 25 roughness checker (Taylor Hobson Precision, USA). Several scans are performed to determine the arithmetic mean deviation roughness (R_a) of the surface.

Fig. 3.6: Measurement of surface roughness by Surtronic 25 roughness checker.

The instrument is calibrated with a standard surface before using it. For this heater surface, the arithmetic mean deviation roughness (R_a) is found to be 1.54 μm. Fig. 3.6 shows the photograph of Surtronic 25 roughness checker.

3.6 Surface Tension Measurements

In this work, a CSC – 70535 DuNouy Precision Tensiometer (CSC Scientific Company, Inc., Fairfax, VA) with a platinum-iridium ring is used for the equilibrium surface tension measurements. This tensiometer uses a fine torsion wire for applying the necessary force required to withdraw the ring from the surface of the liquid under test. Measurements for

sodium oleate solutions are carried out at 28°C. Fig. 3.7 shows the equipment and arrangement for surface tension measurements used in this study.

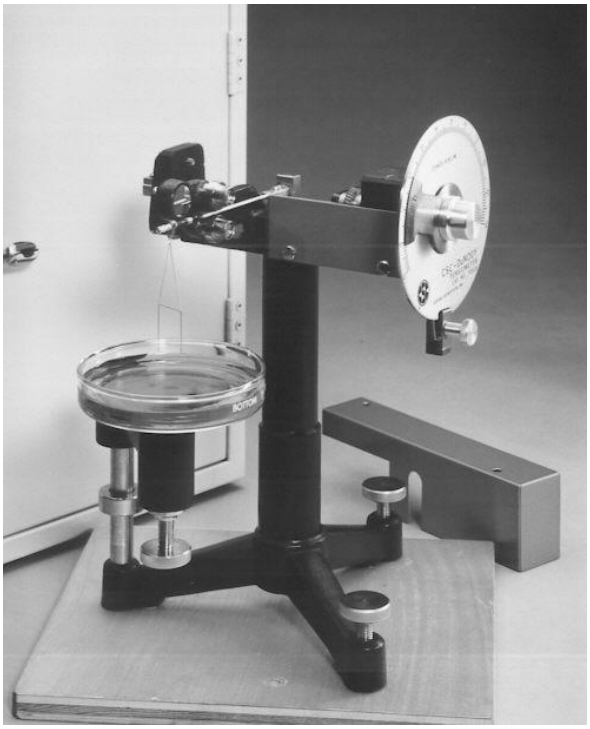

Fig. 3.7: Measurement of surface tension by DuNouy Ring Tensiometer.

The tensiometer is initially calibrated using deionized water at room temperature. Then, by comparing the established value of surface tension of water from literature the validity of measurements are established. All measurements are at 28 °C. The accuracy of the measurements are within ± 0.5 mN/m.

4. RESULTS AND DISCUSSIONS

Saturated nucleate pool boiling heat transfer of water and water with sodium oleate additive are described in this chapter. The results for different concentration solutions are presented, and the optimum enhancement in heat transfer is identified. Results of surface tension measurements for sodium oleate solution are also presented. Discussions of results are also presented in this chapter.

4.1 Boiling of water

The saturated nucleate pool boiling data of water are presented in Fig. 4.1 as a function of heat flux versus the heater excess temperature. Saturated boiling curve of water is compared with the curves generated by other researchers. The boiling curve generated by this study differs from others significantly. This is due to the surface roughness of the heater. Heater surface roughness has a significant impact on the boiling process. The heat transfer coefficient increases with increasing roughness [70]. As heater roughness increases, boiling curve shifts towards left. The heater which is employed in this study has an arithmetic mean deviation roughness of 1.54 μm. Its impact on boiling curve of deionized water is clearly depicted in Fig. 4.1.

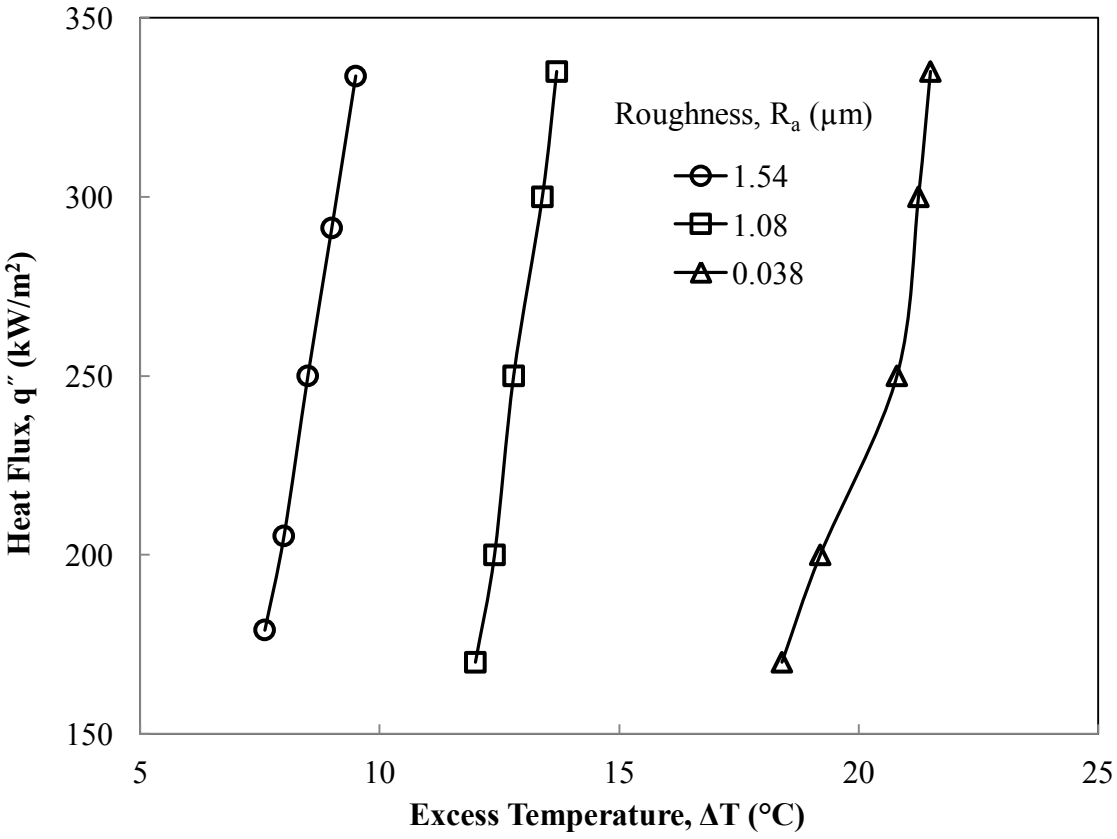

Fig. 4.1: Effect of surface roughness on boiling curve of water (Boiling data for surface roughness of 1.08μm and 0.038μm are adapted from [70]).

Boiling behavior of deionized water is also visually inspected. Photographs of saturated pool boiling of water at different heat flux are shown in Fig. 4.2. Individual bubble regimes as well as column and slug regimes are clearly observed in these photographs.

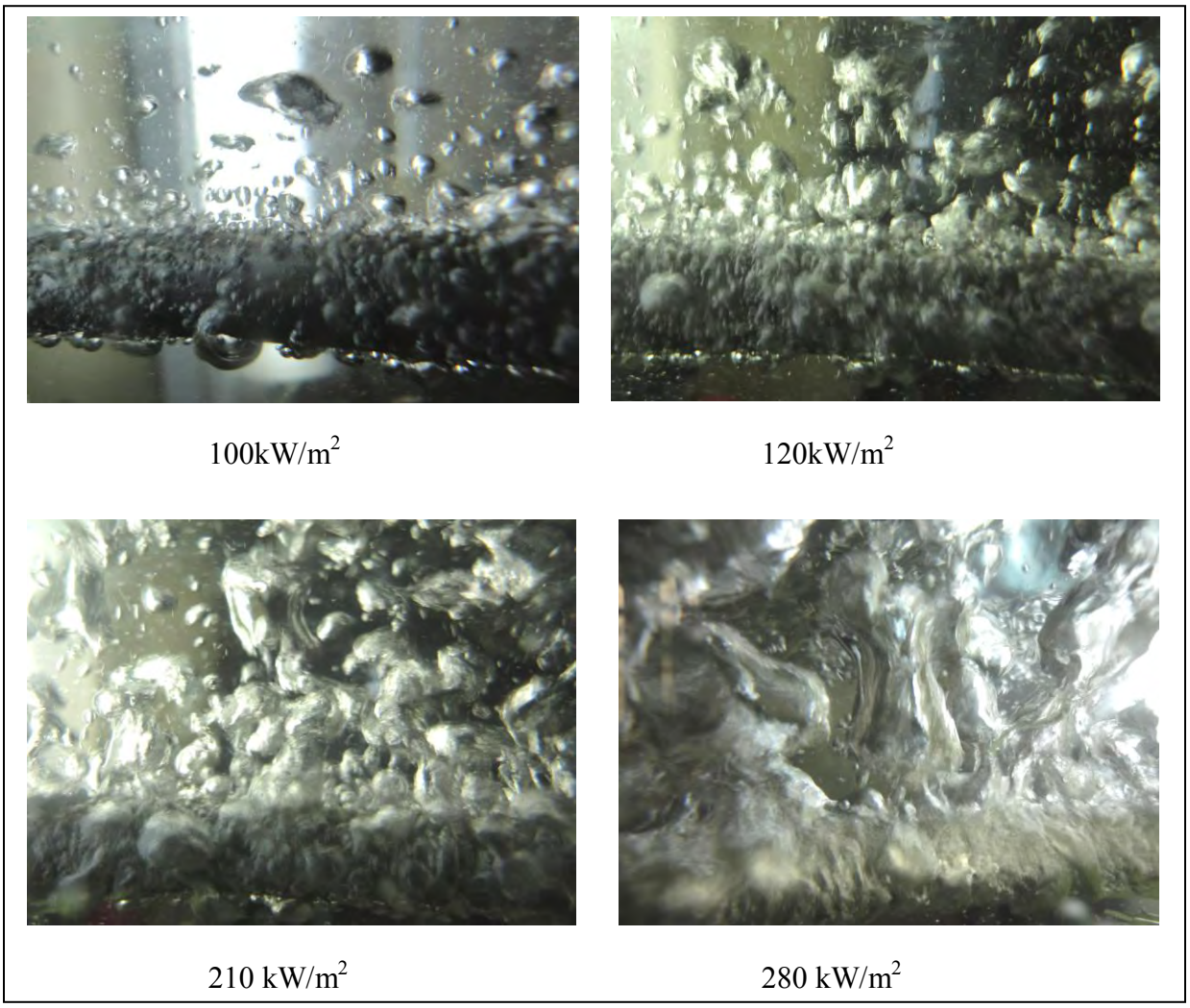

Fig. 4.2: Boiling behavior of deionized water.

4.2 Enhancement

The saturated nucleate pool boiling data for water and water with different concentrations of sodium oleate are plotted in Fig. 4.3. Boiling data of surfactant solutions lie to the left of the boiling curve of pure water, which is an indication of heat transfer enhancement. For increasing and decreasing heat fluxes same measurements of excess temperature are observed.

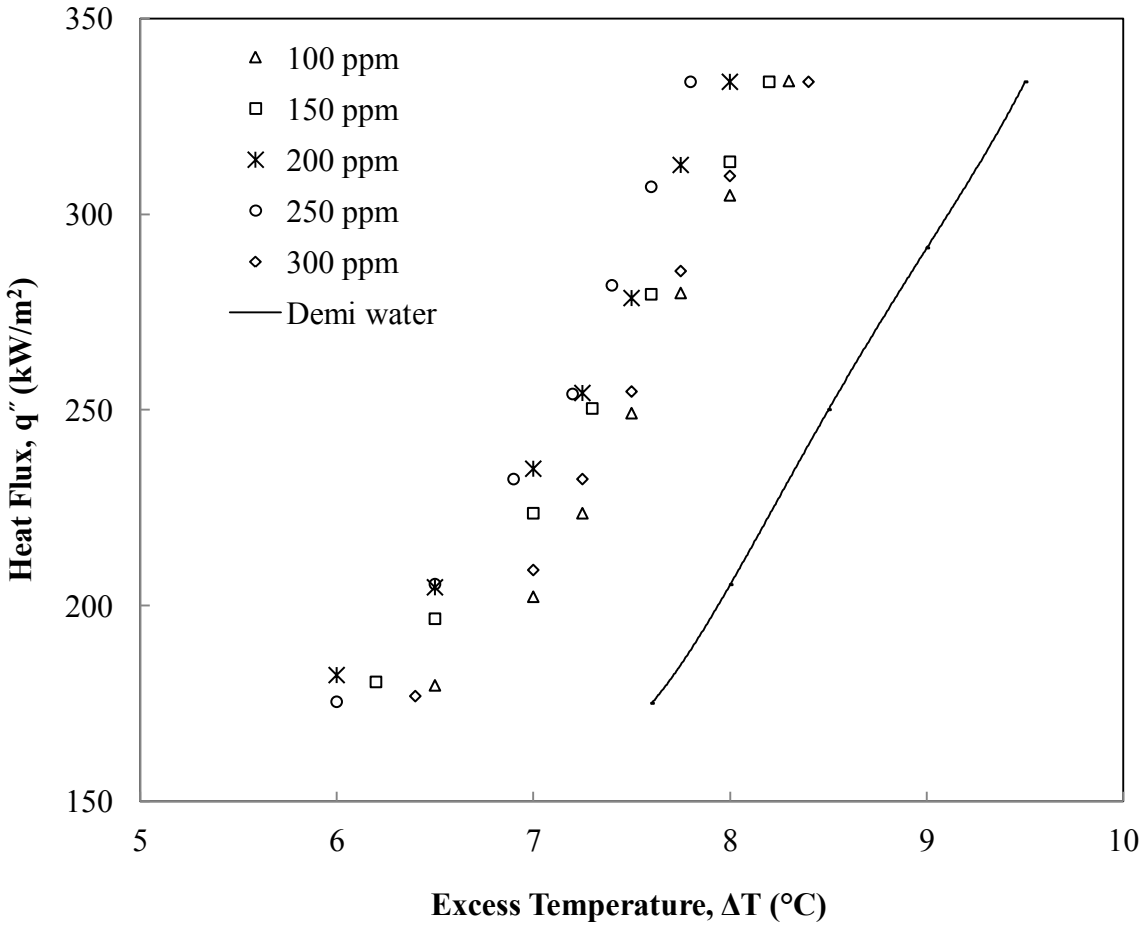

Fig. 4.3: Nucleate Pool boiling data for water and water with sodium oleate at 1 atm.

The influence of heat flux and surfactant concentration on the nucleate pool boiling heat transfer rate of sodium oleate solutions is more evident in Fig. 4.4, where experimental data are expressed as a plot of heat transfer coefficient versus heat flux. The heat transfer increases with increasing the solution concentration, and it reaches maximum when sodium

oleate concentration is 250 ppm. Further addition of surfactant to water decreases the heat transfer coefficient.

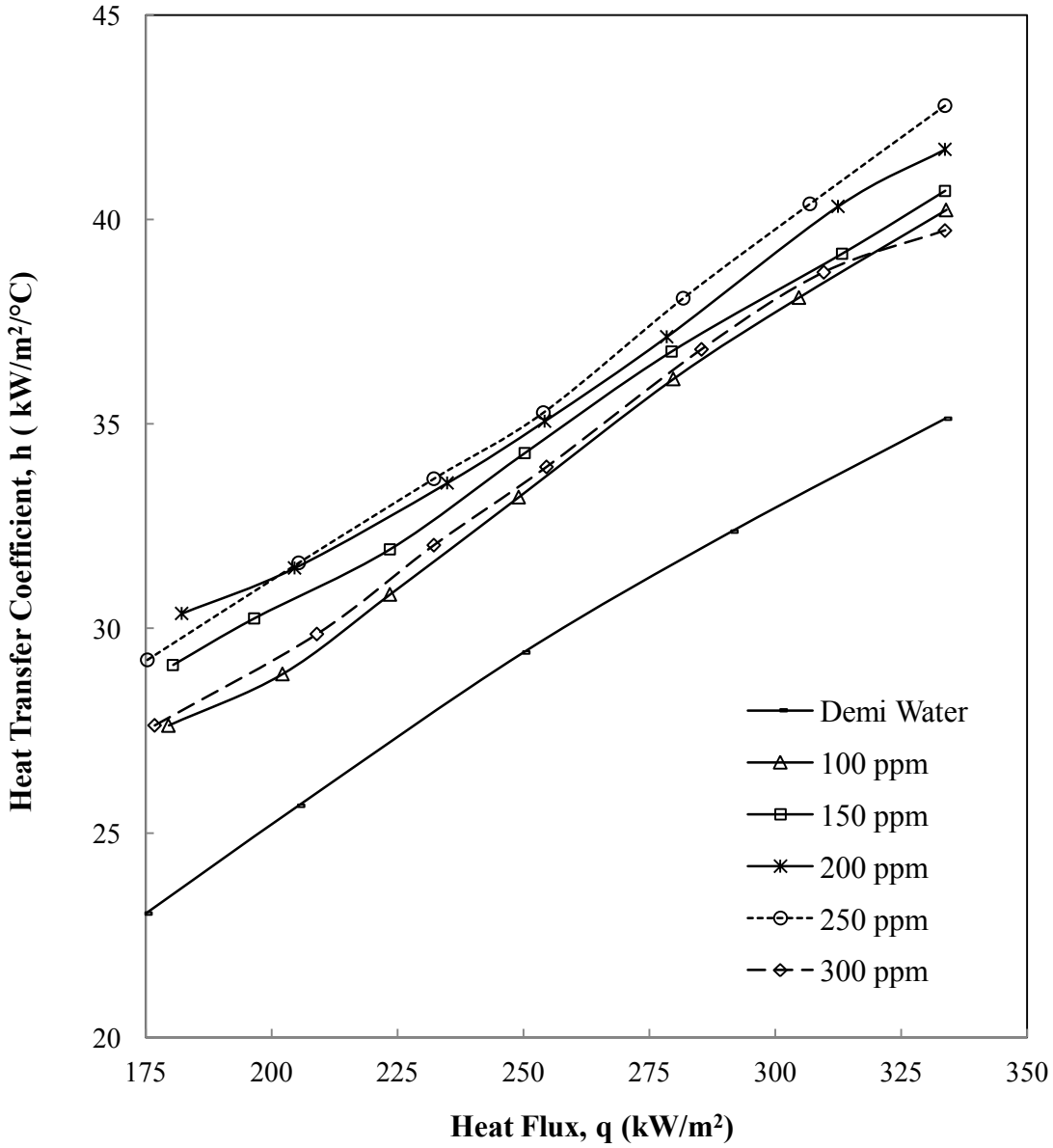

Fig. 4.4: Nucleate boiling heat transfer coefficient as a function of heat flux.

The enhancement of heat transfer by adding surfactant can be shown by the difference, ($h-h_w$), where h and h_w are boiling heat transfer coefficients for surfactant solutions and pure water respectively. ($h - h_w$) as function of surfactant concentration with heat flux as a parameter is shown in Fig. 4.5. The heat transfer coefficient increases with increasing the solution concentration and reaches a maximum value at 250 ppm, and decreases with further increasing the solution concentration.

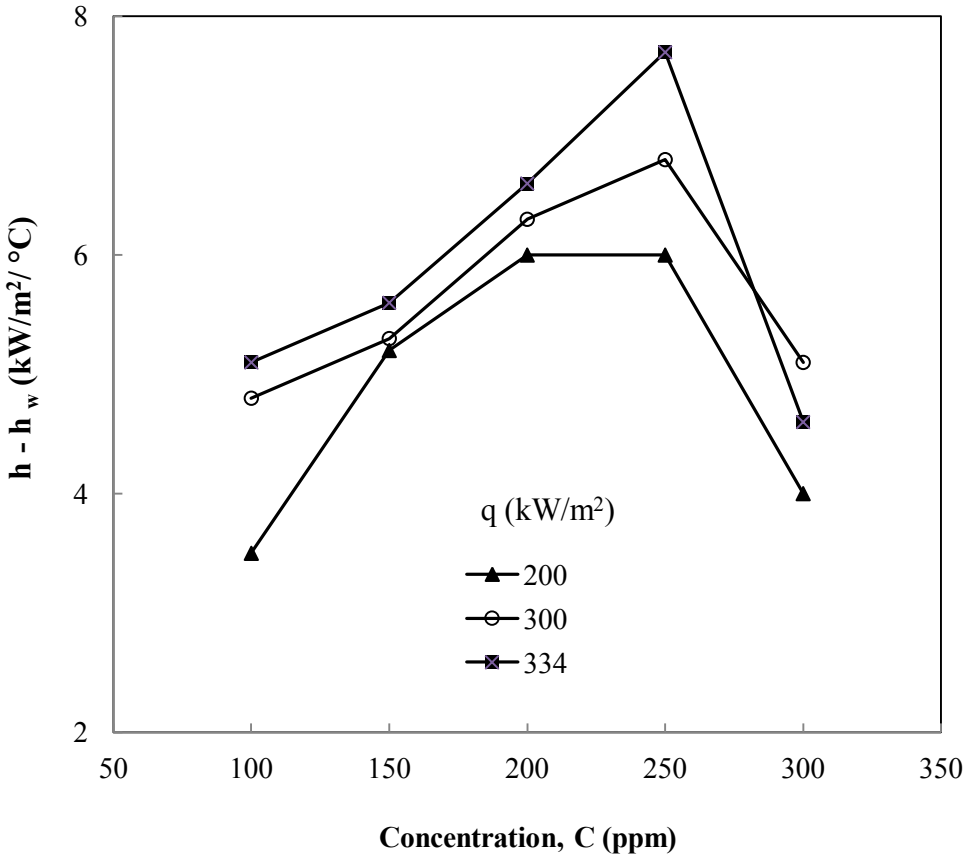

Fig. 4.5: ($h - h_w$) as a function of concentration of sodium oleate solutions.

An explanation for the observed enhancement in pool boiling heat transfer coefficient seen in Fig. 4.5 can be given by considering the effect of equilibrium surface tension of sodium oleate solution. Surface tension data of sodium oleate solution at different concentration is shown in Fig. 4.6.

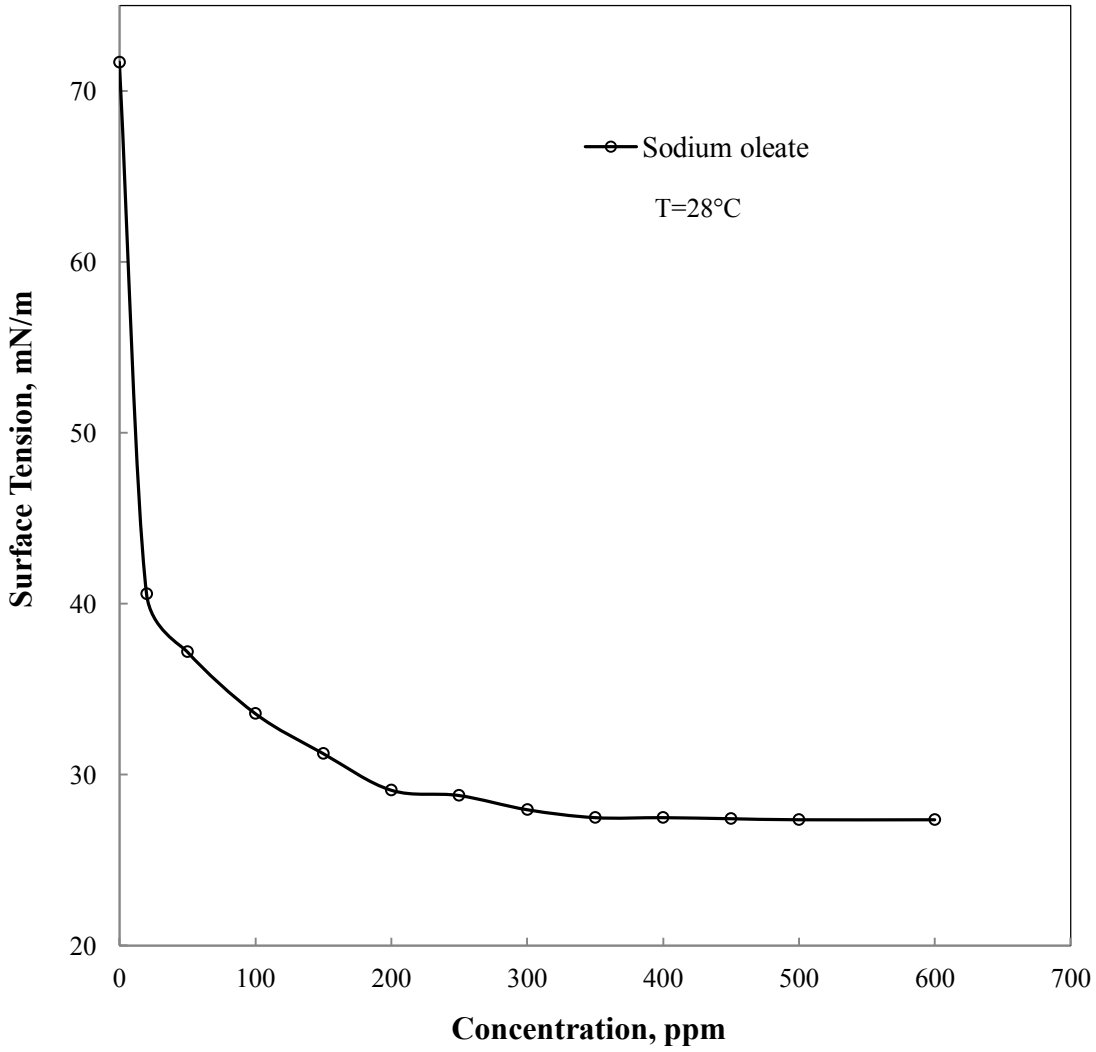

Fig. 4.6: Equilibrium surface tension measurements for Sodium oleate solutions.

It is confirmed that the small decrease in surface tension causes large increase in the number of nuclei [10].

$$n \propto e^{-\sigma^3} \tag{2.18}$$

Eq. (2.18) states that decrease in surface tension increases the rate of nucleus formation which in turn affects the heat transfer rate. But, there are other parameters which are affected by surface tension, such as: bubble growth, bubble departure, bubble shape, etc.

As the surface tension decreases with increasing solution concentration, heat transfer coefficient also increases. There appears to be a critical concentration of 250 ppm, beyond which a reduction in heat transfer coefficient is observed. This concentration appears to be near the cmc of the surfactant. The surfactant behavior in aqueous solution becomes markedly different at or near cmc. This is due to the formation of micelles. The presence of large number of micelles can lead to an increase in apparent viscosity [10].

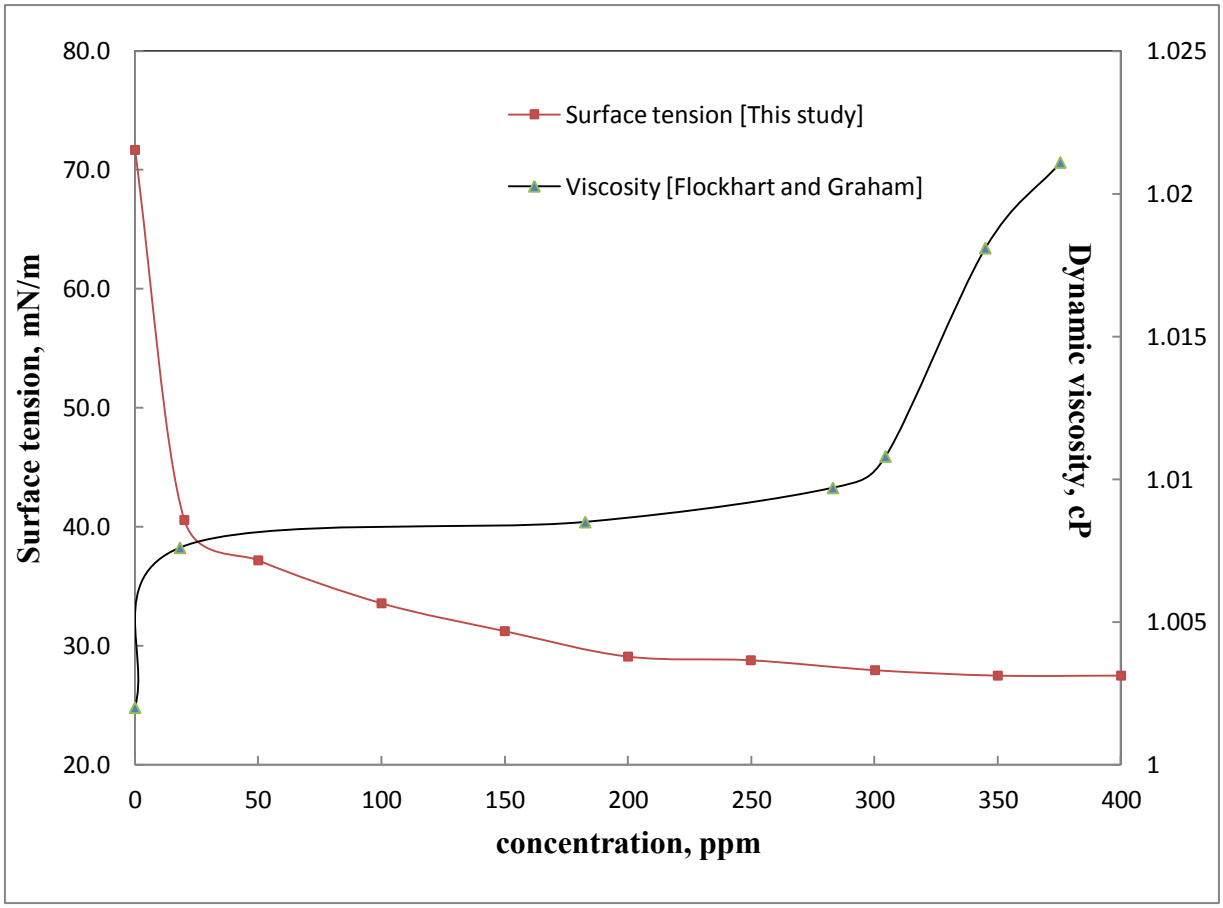

Fig. 4.7: The surface tension (at, 28°C) and, dynamic viscosity (at 20°C) as a function of sodium oleate concentration. (viscosity values are adapted from [71])

Fig. 4.7 is a plot of surface tension and viscosity as a function of surfactant concentration. From this plot it is obvious that beyond 250 ppm the viscosity increases sharply. But, the surface tension depression is nearly absent in this region. The effect of viscosity on heat transfer is discussed in the following text.

Eq. (2.20) is one of the relations which indicate an influence of viscosity on heat transfer coefficient [72].

$$h \propto q^{\ m\ \ \mathrm{n}} \tag{2.20}$$

The value of viscosity exponent ranges from 0 to -1.4.

To explain the joint effect of surface tension and viscosity, the discussion of Marangoni effect is relevant. The phenomenon of liquid flowing along an interface from places with low surface tension to places with a higher surface tension is named after the Italian physicist Marangoni. When gradients in surface tension arise due to concentration differences within one fluid, flow arises as well. The term “Marangoni effect” is also used frequently for a phenomenon that, rather than inducing movement at the interface, retards interfacial motion. Interfaces often contain traces of surface active substances that reduce the surface tension. In general, surface tension lowering solutes adsorb preferentially in the interface (Gibbs adsorption). When, for any reason, an interface expands locally, these surface active solutes are swept outward with the movement, creating a gradient in their concentration. This concentration gradient implies a surface tension gradient which acts opposite to the movement. The interfacial movement is therefore damped. This effect has been referred to as Gibbs elasticity, the Marangoni effect, and, more appropriately, as the Plateau-Marangoni-Gibbs effect.

Consider a fluid zone of thickness d across which the surface tension difference is Δσ. The Marangoni number,

$$Ma\ = \frac{\Delta\sigma.\,\mathrm{d}}{\mathrm{k}} \tag{2.21}$$

is the controlling parameter of interfacial flow driven by the surface tension gradient (Δσ) that affects the heat transfer coefficient [57].

The Marangoni number can also be expressed as,

$$Ma = \mathrm{Re}.\mathrm{Pr} \tag{2.22}$$

Where,

$Re = \frac{\Delta\sigma.\rho d}{^2}$ and $Pr = \frac{c}{k}$ are the Reynolds number and Prandtl number, respectively.

The value of density (ρ), specific heat (c), and thermal conductivity (k) of water and water with surfactant are same as the very small amount of surfactant does not affect these properties. So, the parameters that can change are surface tension and viscosity. From, Fig. 4.7, at low concentration the viscosity almost does not change, so Prandtl number also can not change. But, Reynolds number increases with surface tension depression. Such a behavior of dimensionless number explains the increase in heat transfer coefficient.

But, at higher concentration (beyond 250 ppm of sodium oleate), surface tension depression is ceased to change further, whereas, viscosity increases with increasing surfactant concentration. It increases the Prandtl number proportional by to the viscosity μ, whereas it decreases the Reynolds number proportional by ^{2}. So, the Marangoni effect acts in the opposite direction and suppresses the boiling heat transfer. This explanation is in qualitative agreement with Hetsroni et al. experiments with Habon G surfactant [57].

4.3 Comparison

Our data of transferring maximum amount of heat with a certain concentration of surfactant (250 ppm sodium oleate) is in qualitative agreement with boiling heat transfer data published by Tzan and Yang, and Hetsroni et al. [5,57]. They reported that nucleate boiling heat transfer decreases when the concentration of sodium dodecyl sulfate (SDS) solution was higher than 700 ppm, and when the concentration of Habon G solution was higher than 530 ppm. It can be easily understood from Fig. 4.8.

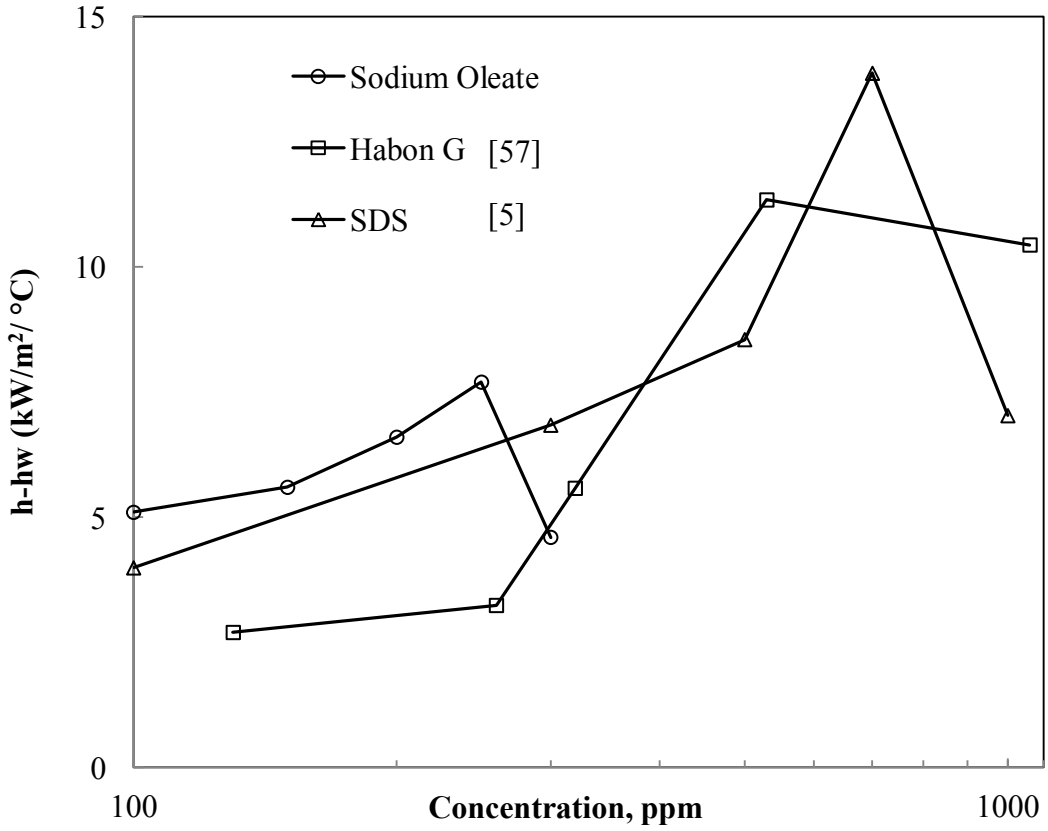

Fig. 4.8: Improvement of heat transfer coefficient for various surfactant solutions as a function of surfactant concentration (Habon G and SDS at 400kW/m^2 [5,57] heat flux and Sodium Oleate at 334kW/m^2).

The heat transfer enhancement for sodium oleate is lower than that of other two surfactant solutions. The reason is that this study used a rough surface which already enhanced the heat transfer coefficient for deionized water. If the heater surface was polished then the enhancement due to surfactant would be more prominent.

In Fig. 4.9 surface tension depression with surfactant concentration for Sodium oleate, Habon G and SDS are plotted. From this figure it is clear that the maximum amount of enhancement is at or near the cmc of these surfactant solutions.

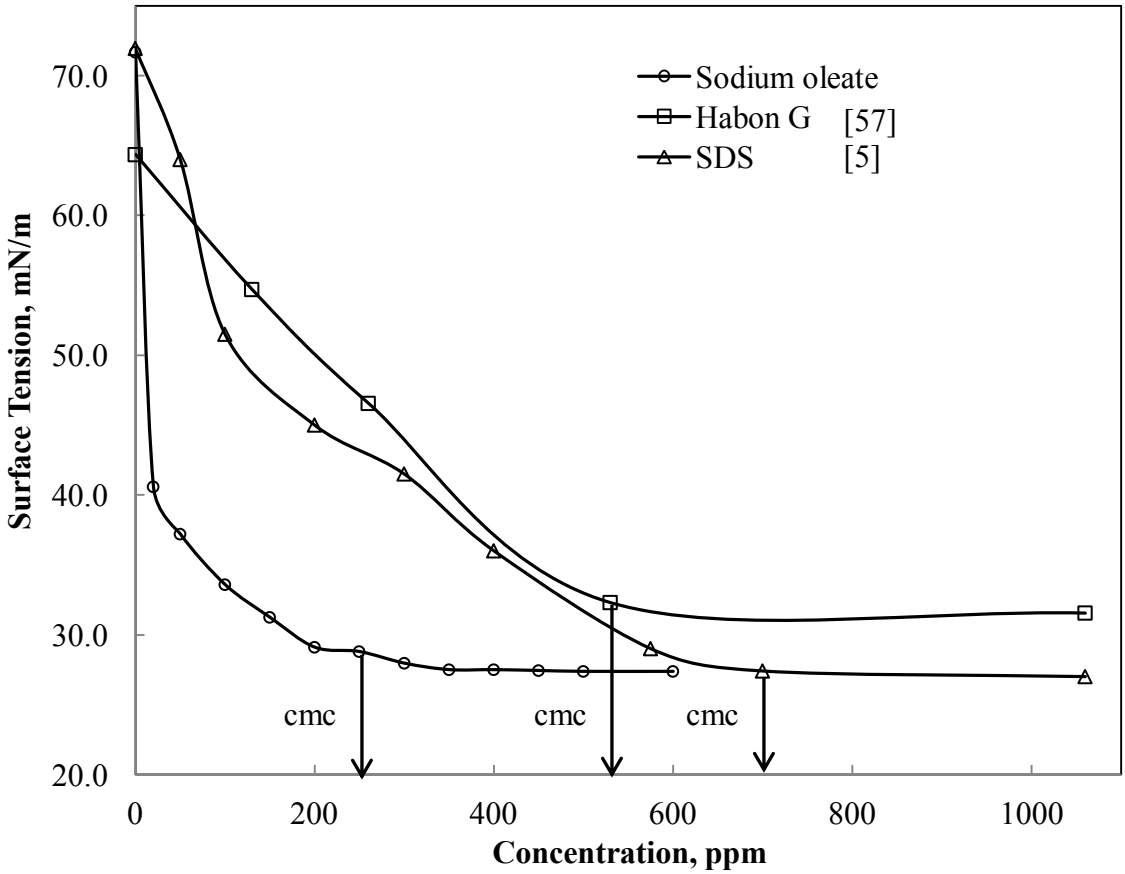

Fig. 4.9: Surface tension versus concentration curves showing approximate critical concentrations (cmc).

To understand the boiling phenomena qualitatively, boiling behavior of water and water with 250 ppm concentration sodium oleate are visualized in Fig. 4.10. The appearance of boiling of water containing surfactant is considerably different with that of deionized water. The surfactant makes the number of vapor bubbles on the heating surface much more. In boiling with surfactant the bubble shape is more regular and difficult to coalesce. The bubbles depart more frequently and are seen to reach the pool free surface where they form a foam layer. The thickness of foam layer is increased with the increases of heat flux.

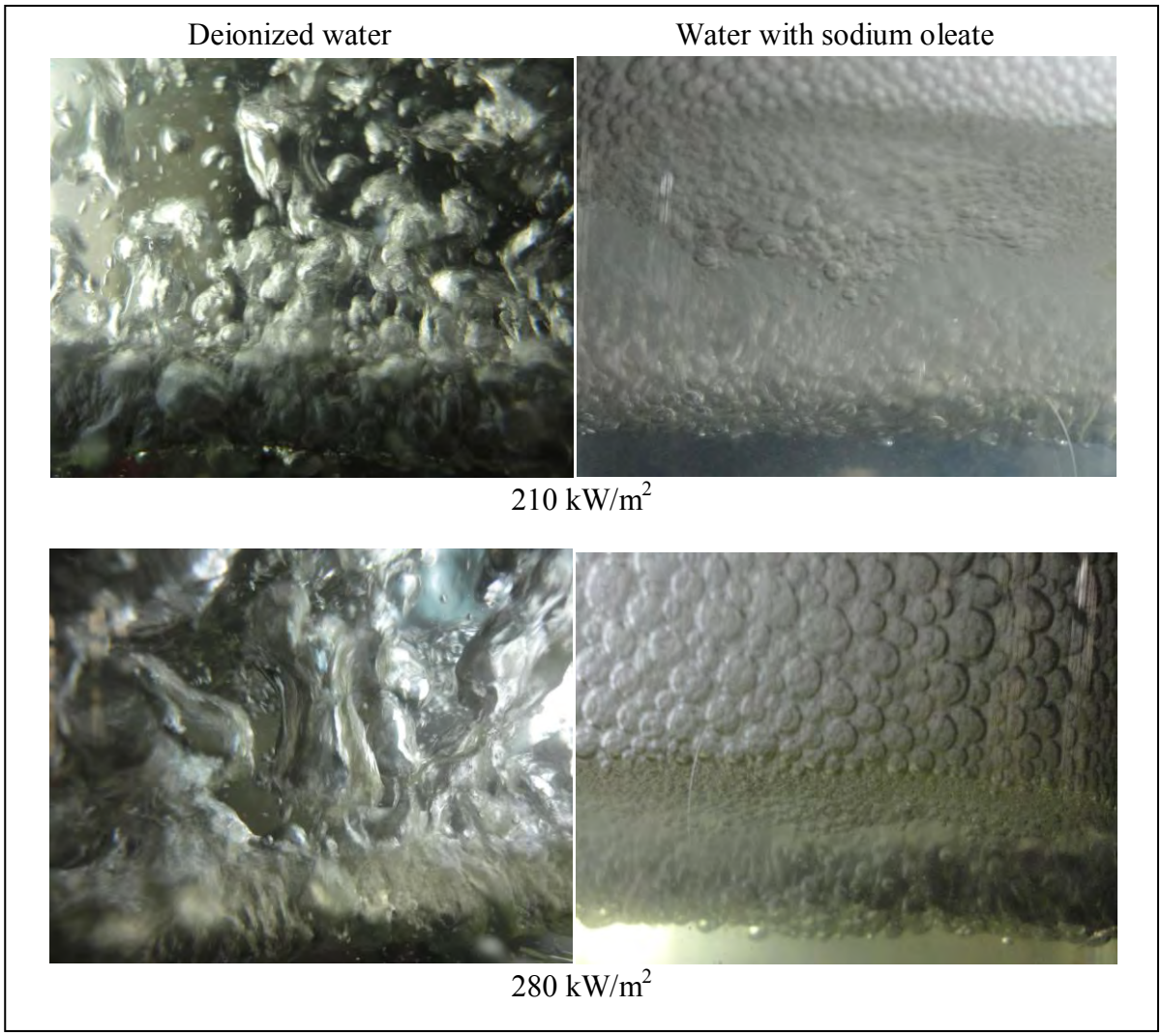

Fig. 4.10: Boiling behavior of deionized water and water with surfactant at 250 ppm concentration.

5. CONCLUSIONS AND RECOMMENDATIONS

5.1 Conclusions

- Pool boiling data of water with sodium oleate surfactant are generated. Addition of a small amount of sodium oleate surfactant enhances the heat transfer rate significantly.
- Maximum heat transfer enhancement occurred at or near the critical micelle concentration. Addition of more sodium oleate beyond this concentration lowers the heat transfer coefficient. This observation validates the results obtained by the previous researcher's by using SDS and Habon G surfactant.
- An attempt to explain enhancement of heat transfer coefficient in presence of sodium oleate in terms of surface tension and viscosity was made. Boiling behavior of water with sodium oleate solution at cmc can be explained qualitatively with these data in terms of Marangoni number. However, it was not conclusive as other parameters such as contact angle, surface tension gradient along the bubble interface etc. may play role in enhancement. Further investigation is needed to understand the phenomenon better.

5.2 Recommendations

- Different surfactant solution can be used to check whether it is possible to explain the heat transfer enhancement with surface tension and viscosity data.
- A data recorder or data logger can be used to get the wall temperature data to see the variation over time.
- A high frame speed scientific camera can be used to photograph and analyze the bubble dynamics which in turn can be used to explain the heat transfer data.

Bibliography

1. Hewitt, G. F., "Boiling" in W. M. Rohsenow, J. P. Hartnett and Y. I. Cho (eds.). *Handbook of Heat Transfer*, chap. 15, pp. 1-168, McGraw-Hill, New York, 1998.

2. Bergles, A. E., Jensen, M. K., and Shome, B., "The Literature of Enhancement of Convective Heat and Mass Transfer," *J. Enhanc. Heat Transfer*, vol. 4, (1-6), 1996.

3. Bergles, A. E., "Some Perspective on Enhanced Heat Transfer-Second Generation Heat Transfer Technology," *J. Heat Transfer*, vol. 110, pp. 1082-1096, 1998.

4. Yang, Y. M., and Maa, J. R., "Pool boiling of dilute surfactant solutions," *ASME Journal of Heat Transfer*, vol. (105), pp. 190-192, 1983.

5. Tzan, Y. L., and Yang, Y. M., "Experimental Study of Surfactant Effects on Pool Boiling Heat Transfer," *ASME Journal of Heat Transfer*, vol. 112, pp. 207-212, 1990.

6. Wasekar, V. M., and Manglik, R. M., "Pool Boiling Heat Transfer in Aqueous Solutions of an Anionic Surfactant," *ASME Journal of Heat Transfer*, vol. 122, pp. 708-715, 2000.

7. Hetsroni, G., Gurevich, M., Mosyak, A., Rozenblit, R., and Segal, Z., "Boiling Enhancement with Environmentally Acceptable Surfactants," *International Journal of Heat and Fluid Flow*, vol. 25, pp. 841-848, 2004.

8. Sephton, H. H., "Upflow Vertical Tube Evaporation of Sea Water with Interface Enhancement; Process Developed by Pilot Plant Testing," *Desalination*, vol. 16, (1), pp. 1-13, 1975.

9. Yang, Y. M., "Boiling Heat Transfer Enhancement by Surfactant Additives," *J. Chin. Inst. Chem. Eng.*, vol. 35, pp. 495-508, 2004.

10. Cheng, L., Mewes, D., and Luke, A., "Boiling Phenomena with Surfactants and Polymeric Additives: A State-of-the-art Review," *International Journal of Heat and Mass Transfer*, vol. 50, pp. 2744-2771, 2007.

11. Collier, J. G., and Thome, J. R., *Covective Boiling and Condensation*, Clarendon Press, Oxford, 1994.

12. Kreith, F., Manglik, R. M., and Bohn, M. S., *Principles of Heat Transfer*, Cengage Learning, Connecticut, 2011.

13. Bergles, A. E., "Elements of Boiling Heat Transfer" in R. T. Lahey (ed.). *Boiling Heat Transfer : Modern Developments and Advances*, pp. 389-446, Elsevier Science Publishers B.V., Amsterdam, 1992.

14. Nukiyama, S., "The Maximum and Minimum Values of Heat Transmitted from Metal to Boiling Water Under Atmospheric Pressure," *J. Japan Soc. Mech. Eng.*, vol. 37, 1934.

15. Drew, T. B., and Mueller, A. C., "Boiling," *AIChE Trans.*, vol. 33, pp. 449-471, 1937.

16. Farber, E. A., and Scorah, E. L., "Heat Transfer to Water Boiling Under Pressure," *Trans. ASME*, vol. 70, pp. 369-384, 1948.

17. Bergman, T. L., Lavine, A. S., Incropera, F. P., and Dewitt, D. P., *Introduction to Heat Transfer*, John Wiley & Sons, Inc., New Jersey, 2011.

18. Engelberg-Forster, K., and Greif, R., "Heat Transfer to a Boiling Liquid - Mechanism and Correlations," *Trans. ASME. Ser. C. J. Heat Transfer*, vol. 81, pp. 43-53, 1959.

19. Lienhard, J. H., and Lienhard, J. H., *A Heat Transfer Textbook*, Phlogiston Press, Massachusetts, 2003.

20. Clark, H. G., Strenge, P. S., and Westwater, J. W., "Active Sites for Nucleate Boiling," *Chemical Engineering Progress Symposium Series*, vol. 55, (29), pp. 103-110, 1959.

21. Tong, L. S., and Tang, Y. S., *Boiling Heat Transfer and Two-Phase Flow*, Taylor & Francis, Washington, D.C., 1997.

22. Hsu, Y. Y., "On the Size Range of Active Nucleation Cavities in a Heating Surface," *Trans. ASME, J. Heat Transfer*, vol. 84, (3), pp. 207-216, 1962.

23. Griffith, P., and Wallis, J. D., "The Role of Surface Conditions in Nucleate Boiling," *AIchE Chem. Eng. Prog. Symp. Ser.*, vol. 56, (30), pp. 49-63, 1960.

24. Bergles, A. E., and Rohsenow, W. M., "The Determination of Forced Convection Surface Boiling Heat Transfer," *Trans. ASME, J. Heat Transfer*, vol. 86, pp. 365-372, 1964.

25. Shai, I. The Mechanism of Nucleate Pool Boiling Heat Transfer to Sodium and the Criterion for Stable Boiling, Massachusetts Institute of Technology, Cambridge, MA, PhD, 1967.

26. Lorentz, J. J., Mikic, B. B., and Rohsenow, W. M. "The Effect of Surface Conditions on Boiling Characteristics". *Proc. 5th Int. heat Transfer Conf.*, New York, Hemisphere, 1974.

27. Mizukami, K., "Entrapment of Vapor in Re-Entrant Cavities," *Letters in Heat and Mass Transfer*, vol. 2, pp. 279-284, 1975.

28. Nishio, S., "Stability of Pre-Existing Vapor Nucleus in Uniform Temperature Field," *Trans. JSME, Series B*, vol. 54, (503), pp. 1802-1807, 1985.

29. Wang, C. H., and Dhir, V. K., "On the Gas Entrapment and Nucleation Site Density During Pool Boiling of Saturated Water," *Journal of Heat Transfer*, vol. 115, pp. 670-679, 1993.

30. Rayleigh, l., "On the Pressure Developed in a Liquid During the Collapse of a Spherical Cavity," *Phil. Mag.*, vol. 34, pp. 94-98, 1917.

31. Plesset, M. S., and Zwick, S. A., "The Growth of Vapour Bubbles in Superheated Liquid," *J. Appli. Phys.*, vol. 25, pp. 493-500, 1954.

32. Mikic, B. B., Rohsenow, W. M., and Griffith, D., "On Bubble Growth Rates," *Int. J. Heat Mass Transfer*, vol. 13, pp. 657-666, 1970.

33. Miyatake, O., Tanaka, I., and Lior, N., "A simple Universal Equation for Bubble Growth in Pure Liquids and Binary Solutions with a Non-Volatile Solute," *Int. J. Heat Mass Transfer*, vol. 40, (1477-1584), 1997.

34. Thome, J. R., "Boiling" in A. Bejan and A. D. Kraus (eds.). *Heat Transfer Handbook*, chap. 9, John Wiley & Sons, Inc., New Jersey, 2003.

35. Hsu, Y. Y., and Graham, R. W. *Transport Processes in Boiling and Two-Phase Systems*, chap. 5 and 6, Hemisphere, New York, 1976.

36. Kast, W., "Significance of Nucleating and Non-stationary Heat Transfer in the heat Exchanger during Bubble Vaporization and Droplet Condensation," *Chem. Eng. Tech.*, vol. 36, (9), pp. 933-940, 1964.

37. Mikic, B. B., and Rohsenow, W. M., "A new correlation of Pool Boiling Data Including the Effect of Heating Surface Characteristics," *Trans. ASME, J. Heat Transfer*, vol. 91, 1969.

38. Han, C. Y., and Griffith, P., "The Mechanism of Heat Transfer in Nucleate Pool Boiling, Part I, Bubble Initiation, Growth, and Departure," *Int. J. Heat Mass Transfer*, vol. 8, (6), pp. 887-904, 1965.

39. Rohsenow, W. M., "A Method of Correlating Heat Transfer Data for Surface Boiling of Liquids," *Trans. ASME*, vol. 74, (969-976), 1952.

40. Berenson, P. J., "Experiments on Pool-Boiling Heat Transfer," *Int. J. Heat Mass Transfer*, vol. 5, pp. 985-999, 1962.

41. Cooper, M. G., "Heat Flow Rates in Saturated Nucleate Pool Boiling: A Wide Ranging Examination Using Reduced Properties" in J. P. Hartnett and T. F. Irvine (eds.). *Advances in Heat Transfer*, vol.16, pp. 157-239, Academic Press, New York, 1984.

42. Gorenflo, D., "Pool Boiling". *VDI-Heat Atlas*, VDI-Verlag, Dusseldorf, Germany, 1993.

43. Bergles, A. E., "Enhancement of Pool Boiling," *Int. J. Refrig.*, vol. 20, (8), pp. 545-551, 1983.

44. Bergles, A. E., "Heat Transfer Enhancement : The Encouragement and Accomodation of High Heat Fluxes, 1995 Max Jakob memorial award lecturer," *J. Heat Transfer*, vol. 119, pp. 8-19, 1997.

45. Bergles, A. E., "Heat Transfer Enhancement - The Maturing of Second Generation Heat Transfer Technology," *Heat Transfer Eng.*, vol. 18, (1), pp. 47-55, 1997.

46. Webb, R. L., and Bergles, A. E., "Heat Transfer Enhancement: Second Generation Technology," *Mech. Eng.*, vol. 115, (6), pp. 60-67, 1983.

47. Thome, J. R., *Enhanced Boiling Heat Transfer*, Hemisphere, New York, 1990.

48. Webb, R. L., and Kim, N. H., *Principles of Enhanced Heat Transfer*, Taylor & Francis, Philadelphia, 2005.

49. Ohardi, M. M., Papar, A. K., and Ansari, A. I., "Some Observations on EHD-Enhanced Boiling of R-123 in the Presence of Oil Contamination" in V. K. Dhir and A. E. Bergles (eds.). *Pool and External Flow Boiling*, pp. 387-396, ASME, New York, 1992.

50. Zaghdoudi, M. C., Cioulachtjian, S., Bonjour, J., and Lallemand, M. "Analysis of Hysteresis and Polarity Influence in Nucleate Pool Boiling Under DC Electric Field". *Proc. EUROTHERM Seminar No. 48: Pool Boiling 2*, Pisa, Italy, Edizioni ETS, 1996.

51. Bonekamp, S., and Bier, K. "Influence of Ultrasound on Pool Boiling Heat Transfer to Mixtures of the Refrigerants R-23 and R-134A". *Proc. EUROTHERM Seminar No. 48: Pool Boiling 2*, Pisa, Italy, Edizioni ETS, 1996.

52. Yang, Y. M., and Maa, J. R., "On the Criteria of Nucleate Pool Boiling Enhancement by Surfactant Addition to Water," *Trans IChemE*, vol. 79, (Part A), pp. 409-416, 2001.

53. Stroebe, G. W., Baker, E. M., and Badger, W. L., "Boiling-Film Heat Transfer Coefficients in a Long-Tube Vertical Evaporator," *Industrial and Engineering Chemistry*, vol. 31, (2), pp. 200-206, 1939.

54. Morgan, A. I., Bromley, L. A., and Wilke, C. R., "Effect of Surface Tension on Heat Transfer in Boiling," *Industrial and Engineering Chemistry*, vol. 41, (12), pp. 2767-2769, 1949.

55. Shibayama, S., Katsuta, M., Suzuki, K., Kurose, T., and Hatano, Y., "A study of Boiling Heat Transfer in a Thin Liquid Film," *Heat Transfer (Japan Research)*, vol. 9, (4), pp. 12-40, 1980.

56. Wasekar, V. M., and Manglik, R. M., "A Review of Enhanced Heat Transfer in Nucleate Pool Boiling of Aqueous Surfactant and Polymeric Solutions," *Journal of Enhanced Heat Transfer*, vol. 6, pp. 135-150, 1999.

57. Hetsroni, G., et al., "The Effect of Surfactants on Bubble Growth, Wall Thermal Patterns and Heat Transfer in Pool Boiling," *International Journal of Heat and Mass Transfer*, vol. 44, pp. 485-497, 2001.

58. Frost, W., and Kippenhan, C. J., "Bubble Growth and Heat Transfer Mechanisms in the Forced Convection Boiling of Water Containing a Surface Active Agent," *Int. J. Heat Mass Transfer*, vol. 10, pp. 931-949, 1967.

59. Kotchaphakdee, P., and Williams, M. C., "Enhancement of Nucleate Pool Boiling with Polymeric Additives," *Int. J. Heat Mass Transfer*, vol. 13, pp. 835-848, 1970.

60. Gannet Jr., H. J., and Williams, M. C., "Pool Boiling in Dilute Non-aqueous polymer solutions," *Int. J. Heat Mass Transfer*, vol. 14, pp. 1001-1005, 1971.

61. Wu, W. T., Yang, Y. M., and Maa, J. R., "Enhancement of Nucleate Boiling Heat Transfer and Depression of Surface Tension by Surfactant Additives," *ASME Journal of Heat Transfer*, vol. 117, pp. 526-529, 1995.

62. Wen, D. S., and Wang, B. X., "Effect of Surface Wettability on Nucleate Pool Boiling Heat Transfer for Surfactant Solutions," *International Journal of Heat and mass Transfer*, vol. 45, pp. 1739-1747, 2002.

63. Westwater, J. W., "Boiling of Liquids" in T. B. Drew and J. W. Hoopes (eds.). *Advances in Chemical Engineering*, vol.1, chap. 1, pp. 1-76, Academic Press Inc., New York, 1956.

64. Lowery, A. J., and Westwater, J. W., "Heat Transfer to Boiling Methanol -Effect of Added Agents," *Industrial and Engineering Chemistry*, vol. 49, (9), pp. 1445-1448, 1957.

65. Zhang, J. Experimental and Computational Study of Nucleate Pool Boiling Heat Transfer in Aqueous Surfactant and Polymer Solutions, University of Cincinnati, Cincinnati, PhD Thesis, 2004.

66. Lange, L. R., *Surfactants: A Practical Handbook*, Hanser Publishers, Munich, 1999.

67. Fainerman, V. B., Mobius, D., and Miller, R., *Surfactant: Chemistry, Interfacial Properties, Applications*, Elsevier Science BV, Amsterdam, 2001.

68. Holmberg, K., Jonsson, B., Kronberg, B., and Lindman, B., *Surfactants and Polymers in Aqueous Solution*, Wiley, New York, 2003.

69. Hunter, R. J., *Foundations of Colloid Science*, Oxford University Press, Oxford, UK, 2001.

70. Jones, B. J., McHale, J. P., and Garimella, S. V., "The influence of surface roughness on nucleate pool boiling heat transfer," *Journal of Heat Transfer*, vol. 131, 2009.

71. Flockhart, B. D., and Graham, H., "Study of Dilute Aqueous Solutions of Sodium Oleate," *Journal of Colloid Science*, vol. 8, (1), pp. 105-115, 1953.

72. Peyghambarzadeh, S. M., Jamialahmadi, M., Alavi Fazel, S. A., and Azizi, S., "Experimental and Theoretical Study of Pool Boiling Heat Transfer to Amine Solutions," *Brazilian Journal of Chemical Engineering*, vol. 26, (1), pp. 33-43, 2009.

73. Holman, J. P., *Heat Transfer*, McGraw-Hill, New York, 2010.

Appendix A

Table A.1: Values of the coefficient C_{sf} in Eq. (2.12) for various liquid-surface combinations [12].

Fluid-heating surface combination	C_{sf}
Water on scored copper	0.0068
Water on emery-polished copper	0.0128
Water-copper	0.0130
Water on emery-polished, paraffin-treated copper	0.0147
Water-brass	0.0060
Water on Teflon coated stainless steel	0.0058
Water on ground and polished stainless steel	0.0080
Water on chemically etched stainless steel	0.0133
Water on mechanically polished stainless steel	0.0132
Water-platinum	0.0130
n-Pentane on lapped copper	0.0049
n-Pentane on emery-rubbed copper	0.0074
n-Pentane on emery-polished copper	0.0154
n-Pentane on emery-polished nickel	0.0127
n-Pentane-chromium	0.0150
Isopropyl alcohol-copper	0.00225
n-Butyl alcohol-copper	0.00305
Ethyl alcohol-chromium	0.0027
Carbon tetrachloride on emery-polished copper	0.0070
Carbon tetrachloride-copper	0.0130
Benzene-chromium	0.0100
50% K_2CO_3-copper	0.00275
35% K_2CO_3-copper	0.0054

Table A.2: Approximate critical heat flux at 1 atm [73].

Fluid-surface combination	q_{max}		
	kW/m^2	$Btu/h.ft^2 \times 10^{-3}$	ΔT_e, °C
Water, copper	620–850	200–270	
Water, Copper-chrome plated	940–1260	300–400	23–28
Water, Steel	1290	410	30
Benzene, copper	130	43.5	
Benzene, Aluminum	160	50.5	
Propanol, nickel-plated copper	210–340	67–110	42–50
Butanol, nickel-plated copper	250–330	79–105	33–39
Ethanol, aluminum	170	55	
Ethanol, Copper	250	80.5	
Methanol, copper	390	125	
Methanol, Chrome-plated copper	350	111	
Methanol, Steel	390	125	

Table A.3: Values of α_0 in W/m^2·K at p_{r0}= 0.1, q_0= 20,000 W/m^2, and R_{p0}= 0.4 µm, with p_{crit} in bar [34].

Methane	46.0	16.04	7,000
Ethane	48.8	30.07	4,500
Propane	42.4	44.10	4,000
n-Butane	38.0	58.12	3,600
n-Pentane	33.7	72.15	3,400
i-Pentane	33.3	72.15	2,500
n-Hexane	29.7	86.18	3,300
n-Heptane	27.3	100.2	3,200
Benzene	48.9	78.11	2,750
Toluene	41.1	92.14	2,650
Diphenyl	38.5	154.2	2,100
Ethanol	63.8	46.07	4,400
n-Propanol	51.7	60.10	3,800
i-Propanol	47.6	60.10	3,000
n-Butanol	49.6	74.12	2,600
i-Butanol	43.0	74.12	4,500
Acetone	47.0	58.08	3,950
R-11	44.0	137.4	2,800
R-12	41.6	120.9	4,000
R-13	38.6	104.5	3,900
R-13B1	39.8	148.9	3,500
R-22	49.9	86.47	3,900
R-23	48.7	70.02	4,400
R-113	34.1	187.4	2,650
R-114	32.6	170.9	2,800
R-115	31.3	154.5	4,200
R-123	36.7	152.9	2,600
R-134a	40.6	102.0	4,500
R-152a	45.2	66.05	4,000
R-226	30.6	186.5	3,700
R-227	29.3	170.0	3,800
RC318	28.0	200.0	4,200
R-502	40.8	111.6	3,300
Chloromethane	66.8	50.49	4,400
Tetrafluoromethane	37.4	88.00	4,750
Hydrogen (on Cu)	12.97	2.02	24,000
Neon (on Cu)	26.5	20.18	20,000
Nitrogen (on Cu)	34.0	28.02	10,000
Nitrogen (on Pt)	34.0	28.02	7,000
Argon (on Cu)	49.0	39.95	8,200
Argon (on Pt)	49.0	39.95	6,700
Oxygen (on Cu)	50.5	32.00	9,500
Oxygen (on Pt)	50.5	32.00	7,200
Water	220.6	18.02	5,600
Ammonia	113.0	17.03	7,000

Appendix B

Sample calculation for wall heat flux

Table B.1: Data for heat flux calculation

Observation No.	Voltage (V)	Current (A)	Electric meter reading (kWh)		Time		Area (m^2)
			Initial	Final	minute	second	
1	160	4	23.64	23.69	4	45	41.89×10^{-4}
2	170	4.2	23.74	23.81	5	55	
3	180	4.4	23.97	24.05	6	8	
4	190	4.6	24.25	24.35	6	48	

In this study, for wall heat flux calculation electric meter readings are used instead of voltmeter – ammeter reading.

For observation No. 1, difference between electric meter reading in 4 minute 45 second is = (23.69-23.64) = 0.05 kWh.

So, the power input is = $\frac{0.05\times3.6\times10^6\ J}{285\ s}$ = 631.57 W

Therefore, heat flux = $\frac{631.57}{41.89\times10^{-4}}$ = 150768.68 W/m^2

Wall heat flux is = 150.8 kW/m^2

Appendix C

Table C.1: Surface tension of sodium oleate solution of different concentration at 28°C.

Concentration, ppm	Surface tension, mN/m
0	71.7
20	40.6
50	37.2
100	33.6
150	31.2
200	29.1
250	28.8
300	28.0
350	27.5
400	27.5
450	27.4
500	27.4
600	27.4

Table C.2: pH of sodium oleate solution at different concentration at 28°C.

Concentration, ppm	pH
0	7.08
20	7.11
50	8.19
100	8.42
150	8.51
200	8.51
250	8.55
300	8.57
350	8.62
400	8.64
450	8.72
500	8.79
600	8.79